PNAS
www.pnas.org

Supplementary Information for

Methylglyoxal-Derived Post-Translational Arginine Modifications are Abundant Histone Marks

James J. Galligan, James A. Wepy, Matthew D. Streeter, Philip J Kingsley, Michelle M. Mitchener, Orrette R. Wauchope, William N. Beavers, Kristie L. Rose, Tina Wang, David A. Spiegel and Lawrence J. Marnett

Email: larry.marnett@Vanderbilt.Edu

This PDF file includes:

Supplemental Methods
Figs. S1 – S40
Datasets S1 – S3
References for SI reference citations

www.pnas.org/cgi/doi/10.1073/pnas.1802901115

Supplemental Methods

Materials and reagents. All reagents were purchased from Sigma Aldrich (St. Louis, MO) unless otherwise indicated. Cell culture media were purchased from Invitrogen (Grand Island, NY). Fetal bovine serum (FBS) was purchased from Atlas Biologicals (Ft. Collins, CO).

Quantification of cellular MGO. Quantification of MGO was achieved using a modified derivatization technique using *o*-phenylenediamine (1). Cells were plated in 6-well plates. Following treatments, the medium was removed and cells washed with ice-cold PBS. Cells were then scraped into ice-cold PBS and pelleted via centrifugation at 1,000 x *g*. Cell pellets were lysed in 100 μL of a buffer containing 150 mM NaCl, 50 mM HEPES (pH 7.4), 1% IGEPAL, and protease and phosphatase inhibitor cocktails and briefly sonicated. Aliquots (10 μL) were removed to quantify protein, and the remaining lysate was mixed 1:1 with ice-cold methanol containing 50 pmol ^{13}C-MGO. Protein was precipitated for 1 h at -20 $^{\circ}$C and pelleted via centrifugation at 20,000 x *g* at 4°C. Supernatants were removed and derivatized with 1 mM *o*-phenylenediamine for 2 h at room temperature protected from light. Samples were centrifuged at 20,000 x *g* and the clarified supernatant was chromatographed using a Shimadzu LC system equipped with a 50 x 2.1 mm, 3 µm particle diameter Ascentis C_{18} column (Supelco, Bellefonte, PA) at a flow rate of 300 µL/min. Buffer A (0.1% formic acid in H_2O) was held at 99% for 0.5 min, then a linear gradient to 98% solvent B (0.1% formic acid in acetonitrile) was applied over the next 4 min. The column was held at 98% B for 2 min and then equilibrated to 99% A for 2 min. Multiple reaction monitoring was conducted in positive ion mode using an AB SCIEX 3200 QTrap with the following transitions: *m/z* 145.1 → 77.1 for MGO; *m/z* 148.1 → 77.1 for ^{13}C-MGO.

Measurement of MGO adducts using QuARKMod – MGO adducts were measured using protein pellets collected from MGO quantification or chromatin samples (50 μg) using previously published methods (2). The following table gives the transitions of all analytes reported here as well as their collision energies (CE).

Species	Q1 (*m*/*z*)	Q3 (*m*/*z*)	CE (V)
Lys	147.1	84.1	22
$^{13}C_6{}^{15}N_2$ Lys	155.1	90.1	22
Arg	175.1	70.1	26
$^{13}C_6{}^{15}N_4$ Arg	185.1	75.1	26
acLys/me_3Lys	189.2	84.1	29
acLys-d_8	197.2	91.1	29
$^{13}C_6{}^{15}N_2$ me_3Lys	197.2	90.1	29
Leu	132.1	86.1	13
$^{13}C_6{}^{15}$N Leu	139.1	93.1	13
meLys	161.1	84.1	26
me_3Lys	175.1	84.1	26
S/ADMA	203.1	70.1	29
meArg	189.1	70.1	29
ADMA-d_7	210.1	77.1	29
MG-H	229.2	70.1	35
MG-H-^{13}C	230.2	70.1	35
CEA	247.2	70.1	47
CEA-^{13}C	248.2	70.1	47
CEL	219.2	84.1	29
CEL-d_4	223.2	88.1	29

Measurement of GLO1 activity. GLO1 activity was quantified via incubation of cell lysate (100 μg protein) with a mix of 2.5 mM GSH and 2.5 mM MGO (pre-incubated at 37ºC for 1 h to generate hemithioacetal substrate) at 37ºC for 30 min. 5 nmol of stable isotopte-labeled GSH-(glycine-$^{13}C_2$,^{15}N) was then added to each reaction as the internal standard and reactions were immediately quenched via addition of ethyliodoacetate (200 mM in acetonitrile (ACN), 20 mM final). Samples were derivatized for 30 min at room temperature protected from light. Protein was precipitated via addition of 20% (w/v) 5-sulfosalicylic acid (2% final) and removed via centrifugation at 10,000 x *g* for 5 min at room temperature. Supernatants were removed and diluted 1:1 in H_2O containing 200 mM heptafluorobutyric acid (HFBA). Clarified supernatant (20 μL) was chromatographed using a Shimadzu LC system equipped with a 50 x 2.1 mm,

2.6 μm particle diameter Kintetix C_8 column (Phenomenex, Torrance, CA) at a flow rate of 400 μL/min. Solvent A (10 mM HFBA in H_2O) was held at 96% for 0.5 min, then a linear gradient to 95% B (10 mM ACN) was applied over the next 4.5 min. The column was held at 95% B for 0.5 min and then equilibrated to 96% A for 2 min. The needle was washed prior to each injection with a buffer consisting of 25 mM NH_4OAc in MeOH. Multiple reaction monitoring was performed in positive ion mode using an AB SCIEX 3200 QTrap with the following transitions: *m/z* 394.2 □ 265.2 for GSH; *m/z* 380.1 □ 233.1 for LGSH; 397.2 □ 268.2 for GSH-(glycine-$^{13}C_2$,^{15}N). GSH and LGSH were quantified using GSH-(glycine-$^{13}C_2$,^{15}N).

Assessment of MGO toxicity. Cells were seeded in 96-well plates at a density of 3×10^3 and allowed to adhere overnight. The following day, adherent cells were treated with either sterile-filtered ddH_2O or MGO. After 24 h, viability was determined using WST-1 (Roche Applied Science) according to the manufacturer's protocol.

SDS-PAGE and immunoblotting. Samples were denatured in SDS loading buffer and heated at 95°C for 5 min. Proteins were resolved via 15% SDS-PAGE and transferred to nitrocellulose membranes (BioRad, Hercules, CA). Membranes were blocked with Odyssey Blotting Buffer (Li-Cor Biosciences, Superior, NE) for 30 min at room temperature. Primary antibodies were incubated with membranes overnight at 4 °C with the following dilutions: GLO1 (1:2500, Millipore: 05-1925); GLO2 (1:2000, ThermoFisher: PA5-30965); DJ-1/PARK7 (1:2000, Abcam, ab18257); Actin (Santa Cruz, sc-1616, 1:5000); MG-H1, MG-H2, and MG-H3/CEA (1:1000, laboratory of D.A.S., (3)); H2B (1:5000, CST: #2934); H3 (1:5000, CST: #3638); H2A (1:5000, CST: #3636); H4 (1:2000, CST: #2935); H3K4me (1:5000, Abcam: ab8895); $H3K27me_3$ (1:10000, Millipore: 07-449); H3K27ac (1:2000, Abcam: ab4729); H3K56ac (1:1000, Abcam: ab71956); $H3K79me_2$ (1:2000, Abcam: ab3594); H2BK5ac (1:2000, Abcam: ab40886); H2BK12ac (1:2000, Abcam: ab40883); H2BK15ac (1:2000, Abcam: ab62335); H2BK20ac (1:2000, CST: 2571); H2BK120ub (1:2000, CST: #5546); H4K5ac (1:2000, CST: #8647); H4K8ac (1:2000, CST: #2594); H4K12ac (1:2000, CST: #13944); H2AK5ac (1:1000, Abcam: ab45152); H2AK9ac (1:1000,

Abcam: ab47816). Following 3 washes with Tris-buffered saline (TBS) + 0.1% Tween-20 (TBST), infrared secondary antibodies (Li-Cor) were added in blocking buffer (1:5000) for 45 min. Blots were developed following 3 additional washes with TBST using the Odyssey Infrared Imaging System (Li-Cor).

Synthesis of stably-labeled MG-H isomers. ^{13}C-Labeled methylglyoxal hydroimidazolone (MG-H) standards were synthesized as previously reported with the incorporation of ^{13}C-labeled reagents into the synthetic route (4). Specifically, MG-H1 and MG-H3 were labeled via the incorporation of 1-^{13}C-DL-alanine (Cambridge Isotope Laboratories), while MG-H2 was labeled via the incorporation of ^{13}C-thiourea (Cambridge Isotope Laboratories).

Proteomic characterization of histone adducts. Chromatin (5 μg) was separated on a 15% SDS-PAGE gel and stained with SimplyBlue SafeStain (Invitrogen, Carlsbad, CA). Four gel bands were excised corresponding to each histone based on molecular weight. Bands were reduced, alkylated, and destained as described (5). To obtain 100% sequence coverage over all four histones, samples were digested and peptides were extracted as previously described (6). Peptides were reconstituted in 0.1% formic acid, and peptide mixtures were loaded onto a capillary reverse-phase analytical column (360 μm o.d. x 100 μm i.d.) using an Dionex Ultimate 3000 nanoLC and autosampler. The analytical column was packed with 22 cm of C18 reverse-phase material (Jupiter, 3μm beads, 300 Å or Aqua C18, 3 μm beads, Phenomenex), directly into a laser-pulled emitter tip. Peptides were gradient-eluted at a flow rate of 400 nL/min, and the mobile phases consisted of water containing 0.1% formic acid (solvent A) and acetonitrile containing 0.1% formic acid (solvent B). A 90 min gradient was performed, consisting of the following: 0–3 min, 1% B (during sample loading); 3–68 min, 1–40% B; 68–77 min, 40–95% B; 77-78 min, 95% B; 78-79 min 95–2% B; and 79–90 min, 2% B (column re-equilibration). Upon gradient elution, peptides were mass analyzed on an Q Exactive Plus mass spectrometer (Thermo Scientific), equipped with a nanoelectrospray ionization source. The instrument was operated using a data-dependent method with dynamic exclusion enabled. Full-scan (*m/z* 375–1800) spectra were acquired with the Orbitrap (resolution

60,000). The instrument method consisted of MS1 using an MS AGC target value of 3e6, followed by up to 20 MS/MS scans of the most abundant ions detected in the preceding MS scan. A maximum MS/MS ion time of 100 ms was used with a MS2 AGC target of 1e5. Dynamic exclusion was set to 15s, HCD collision energy was set to 27 nce, and peptide match and isotope exclusion were enabled.

For identification of histone peptides, tandem mass spectra were searched with Sequest (Thermo Fisher Scientific) against a human subset database created from the UniprotKB protein database (www.uniprot.org). Due to the plethora of diverse histone modifications, multiple database searches were required for each sample to minimize false positives. These variable modifications included: +57.0214 (carbamidomethylation) on Cys; +15.9949 (oxidation) on Met; +14.0157 (methylation), +28.0313 (dimethylation), +42.0106 (acetylation) on Lys; +54.0106 (MG-H) on Arg; +72.0212 (CEL, CEA) on Lys and Arg. Additionally, a variable mass of +56.0262 (propionylation) was applied to Lys where propionylation was required. Search results were assembled using Scaffold 3.0 or 4.3.2 (Proteome Software). Spectra of interest were inspected using Xcalibur 2.2 Qual Browser software (Thermo Scientific). Tandem mass spectra of all modified peptide precursors as well as spectra acquired of the corresponding unmodified peptide forms were interrogated manually.

RNA-Sequencing analysis. WT or GLO1$^{-/-}$ cells (4 x 10^6) were treated with either vehicle (ddH_2O), 50 μM MGO or 500 μM MGO for 6 h. Following treatments, cells were washed once with ice-cold PBS and then scraped and pelleted. Cell pellets were placed in a QIAshredder column and total cellular RNA was extracted using a commercial RNA purification kit (RNeasy, Qiagen, Valencia, CA), according to manufacturer's instructions. Total RNA quality was assessed at the Vanderbilt Technologies for Advanced Genomics (VANTAGE) core facility using the 2100 Bioanalyzer (Agilent). At least 200ng of DNase-treated total RNA with an RNA integrity number greater than 6 was used to generate polyA (mRNA) enriched libraries using Stranded mRNA sample kits with indexed adaptors (New England BioLabs). Library quality was assessed using the 2100 Bioanalyzer (Agilent) and libraries were quantitated using KAPA Library Quantification Kits (KAPA Biosystems). Pooled libraries were subjected to 150 bp

paired-end sequencing according to the manufacturer's protocol (Illumina NovaSeq6000). Bcl2fastq2 Conversion Software (Illumina) was used to generate de-multiplexed Fastq files. Reads were trimmed to remove adapter sequences using Cutadapt v1.16 (7) and aligned to the human b37 genome using STAR v2.5.3a at the Vanderbilt Technologies for Advanced Genomics Analysis and Research Design (VANGARD) (8). Ensembl v75 gene annotations were provided to STAR to improve the accuracy of mapping. Quality control on both raw reads and adaptor-trimmed reads was performed using FastQC (www.bioinformatics.babraham.ac.uk/projects/fastqc). featureCounts v1.15.2 (9) was used to count the number of mapped reads to each gene. Significantly differential expressed genes with FDR-adjusted p-value < 0.05 and absolute fold change > 2.0 were detected by DESeq2 (v1.18.1) (10).

References

1. Chaplen FW, Fahl WE, & Cameron DC (1996) Method for determination of free intracellular and extracellular methylglyoxal in animal cells grown in culture. *Analytical biochemistry* 238(2):171-178.
2. Galligan JJ, *et al*. (2016) Quantitative Analysis and Discovery of Lysine and Arginine Modifications (QuARKMod). *Anal. Chem*.
3. Wang T, Streeter MD, & Spiegel DA (2015) Generation and characterization of antibodies against arginine-derived advanced glycation endproducts. *Bioorganic & medicinal chemistry letters* 25(21):4881-4886.
4. Wang T, Kartika R, & Spiegel DA (2012) Exploring post-translational arginine modification using chemically synthesized methylglyoxal hydroimidazolones. *Journal of the American Chemical Society* 134(21):8958-8967.
5. Aluise CD, *et al*. (2013) Peptidyl-prolyl cis/trans-isomerase A1 (Pin1) is a target for modification by lipid electrophiles. *Chemical research in toxicology* 26(2):270-279.
6. Galligan JJ, *et al*. (2014) Stable Histone Adduction by 4-Oxo-2-nonenal: A Potential Link between Oxidative Stress and Epigenetics. *Journal of the American Chemical Society*.
7. Martin M (2011) Cutadapt removes adapter sequences from high-throughput sequencing reads. *EMBnet.journal* 17:10-12.
8. Dobin A, *et al*. (2013) STAR: ultrafast universal RNA-seq aligner. *Bioinformatics* 29(1):15-21.
9. Liao Y, Smyth GK, & Shi W (2014) featureCounts: an efficient general purpose program for assigning sequence reads to genomic features. *Bioinformatics* 30(7):923-930.
10. Love MI, Huber W, & Anders S (2014) Moderated estimation of fold change and dispersion for RNA-seq data with DESeq2. *Genome Biol* 15(12):550.

Datasets

Dataset S1. gRNA and primer design for the generation of HEK293 cells lacking *GLO1*. The gRNA utilized was designed to target the Bae1 restriction enzyme target site. The GLO1 gene was amplified via PCR using the forward and reverse primers listed. RFLP was then performed via PCR product treatment with Bae1 and GLO1 knockout cell lines determined based upon the absence of the restriction fragments shown.

Dataset S2. Protein-coding transcripts significantly altered in GLO1$^{-/-}$ cells treated with either vehicle, 50 μM, or 500 μM MGO for 6 h.

Dataset S3. DAVID analysis was performed on each gene list, revealing pathways and gene ontology enrichments for each cohort.

Supplemental Figures

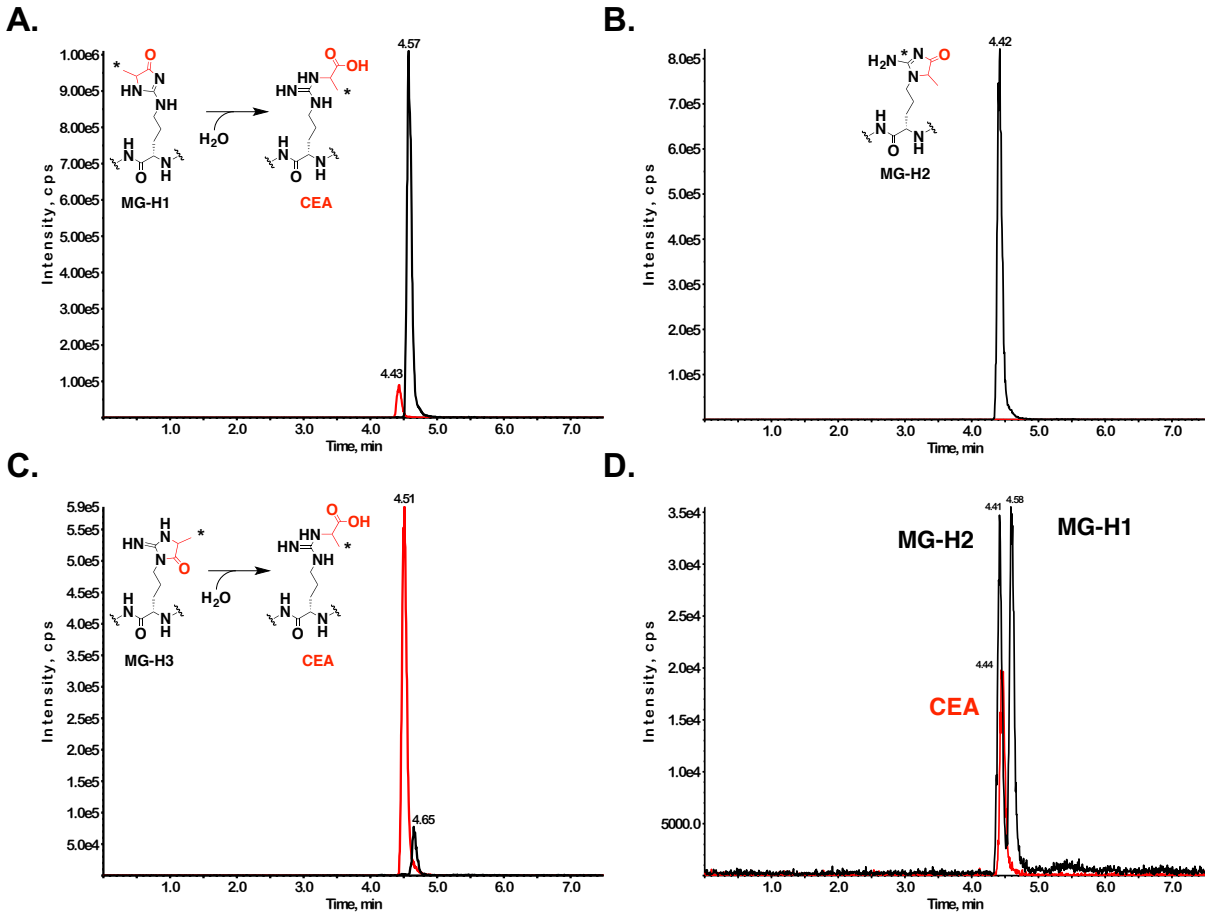

Fig. S1. Stably labeled MG-H1 (A), MG-H2 (B), and MG-H3 (C) internal standards are chromatographically resolved using QuARKMod. * indicates the presence of a ^{13}C. MG-H3 (Black) is readily hydrolyzed to generate CEA (Red) following a 24 h incubation at 37°C, whereas < 10% CEA results from MG-H1 hydrolysis. (D) MG-H1, MG-H2, MG-H3 were mixed at an equimolar ratio to demonstrate chromatographic separation of the MG-H isomers.

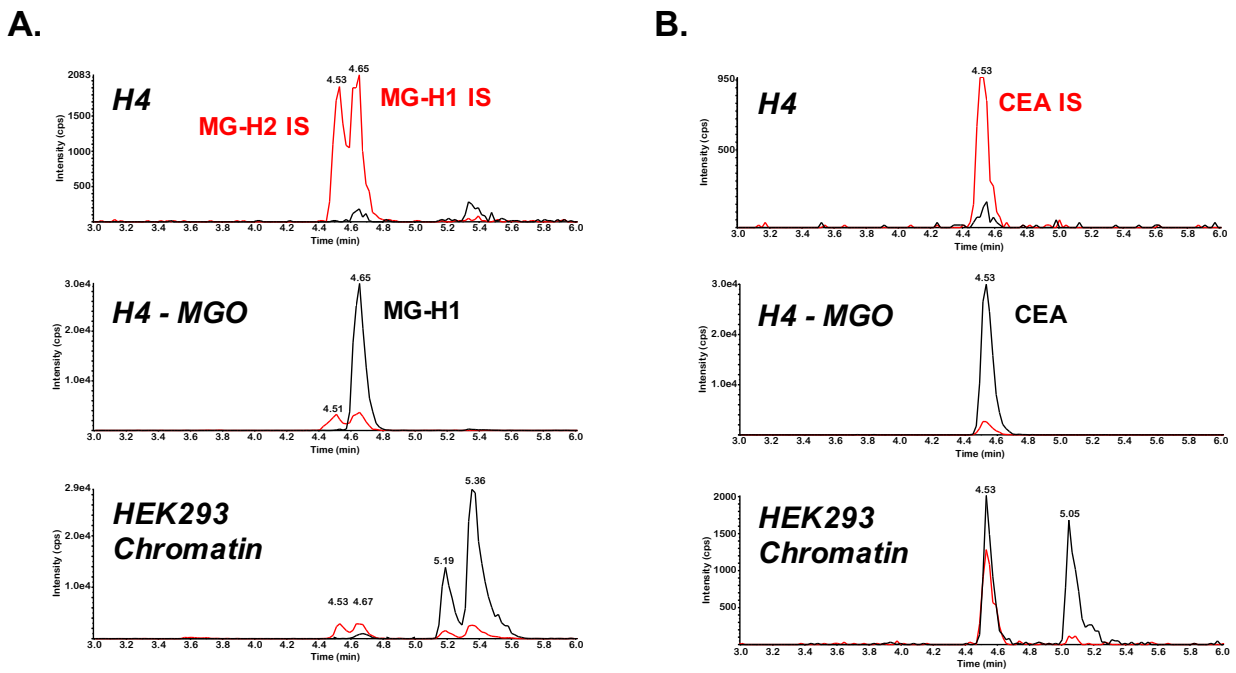

Fig. S2. (A) Levels of MG-H1 detected in untreated histone H4 (top), histone H4 reacted with 100 μM MGO for 24 h (center), and chromatin from untreated HEK293 cells (bottom). In each case, the sample data are shown in black and the internal standard in red. MG-H1 in untreated H4 was below the limits of detection of the assay, but the adduct was readily detected following MGO treatment. In chromatin, peaks are detected (5.19 and 5.36 min) with the same MRM transitions as MG-H1, these peaks do not co-elute with the internal standards. (B) Similar results are observed upon assay for CEA.

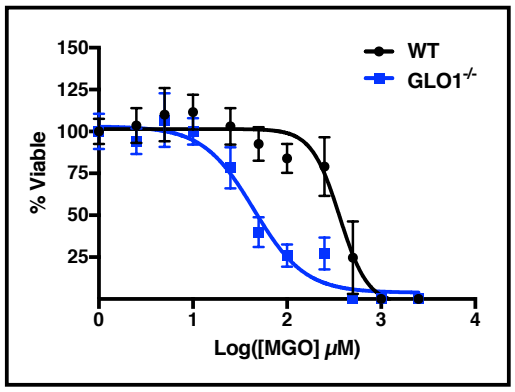

Fig. S3. GLO1$^{-/-}$ cells display a significant shift decrease in viability (compared to WT cells) following exposure to MGO for 24 h. Data are presented as the mean ± S.D. of twenty-four measurements.

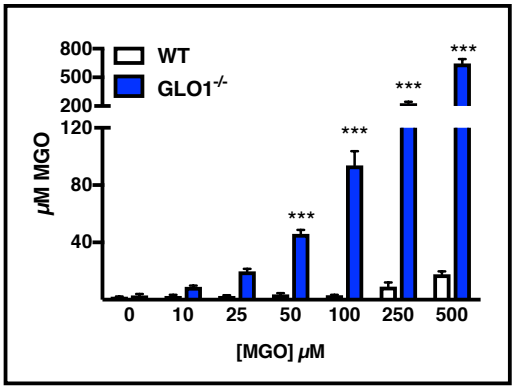

Fig. S4 Cellular MGO was quantified in WT and GLO1$^{-/-}$ cells exposed to increasing concentrations of MGO for 1 h. Measurements were performed in triplicate and are presented as the mean ± S.D. Statistical significance was determined using an unpaired t-test (*** $p < 0.001$).

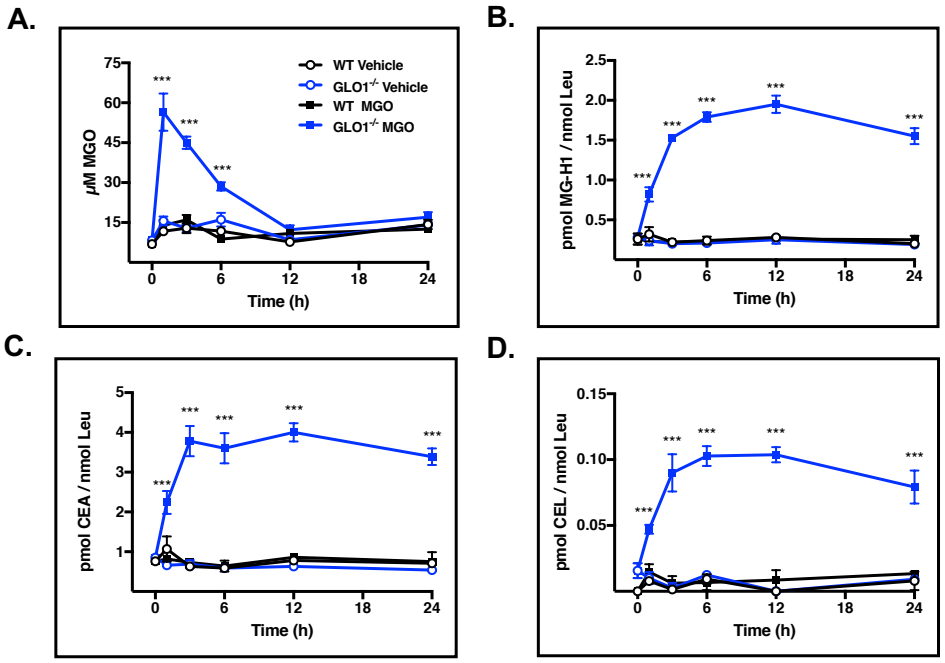

Fig. S5. (*A*) Cellular MGO was quantified over time in WT and GLO1$^{-/-}$ cells exposed to 50 μM MGO. Measurements were performed in triplicate and are presented as the mean ± S.D. (*B-D*) Protein pellets collected from cells described in (*A*) were analyzed for MGO-derived PTMs using QuARKMod. GLO1$^{-/-}$ cells display increased MGO-derived PTMs following exposure to 50 μM MGO with concentrations peaking at ~ 6 h. Statistical significance was determined by two-way ANOVA (*** $p < 0.001$).

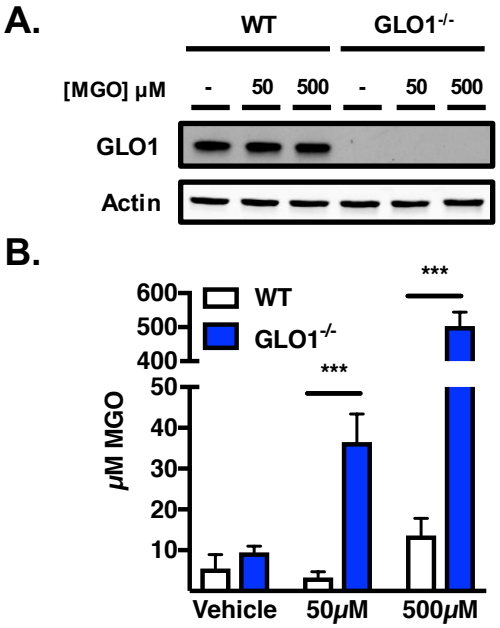

Fig. S6. (A) GLO1 is not altered following treatment with either 50 or 500 μM MGO for 6 h. (B) Cellular MGO is significantly elevated in GLO1$^{-/-}$ cells 6 h post-MGO exposure. Data are presented as the mean ± S.D, N = 3 and statistical significance was determined by a two-way ANOVA (*** $p < 0.001$).

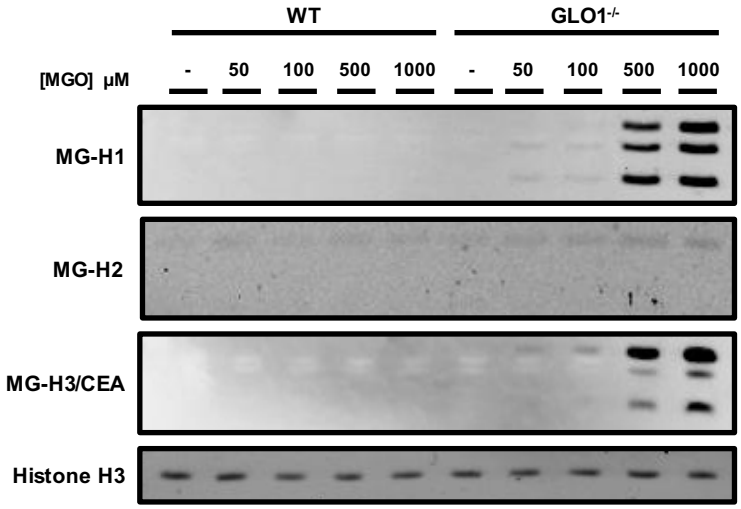

Fig. S7. WT or GLO1$^{-/-}$ cells were treated with increasing concentrations of MGO for 6 h. Chromatin was harvested and subjected to immunoblotting. A concentration-dependent increase in MG-H1 and MG-H3/CEA immunostaining is observed in GLO1$^{-/-}$ cells while MG-H2 is not observed.

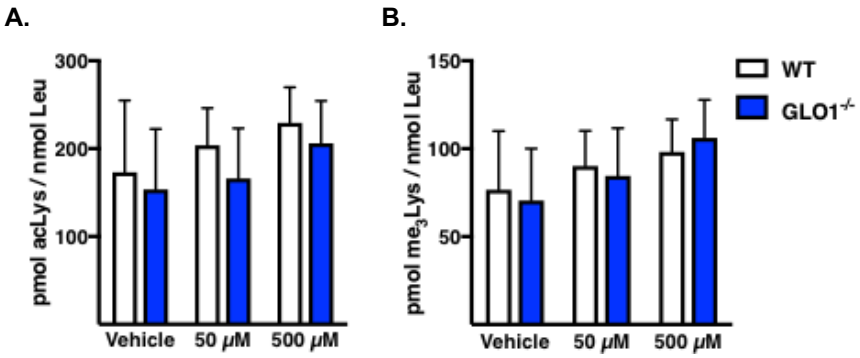

Fig. S8. QuARKMod demonstrates the levels of chromatin (*A*) acLys and (*B*) me_3Lys in each cohort.

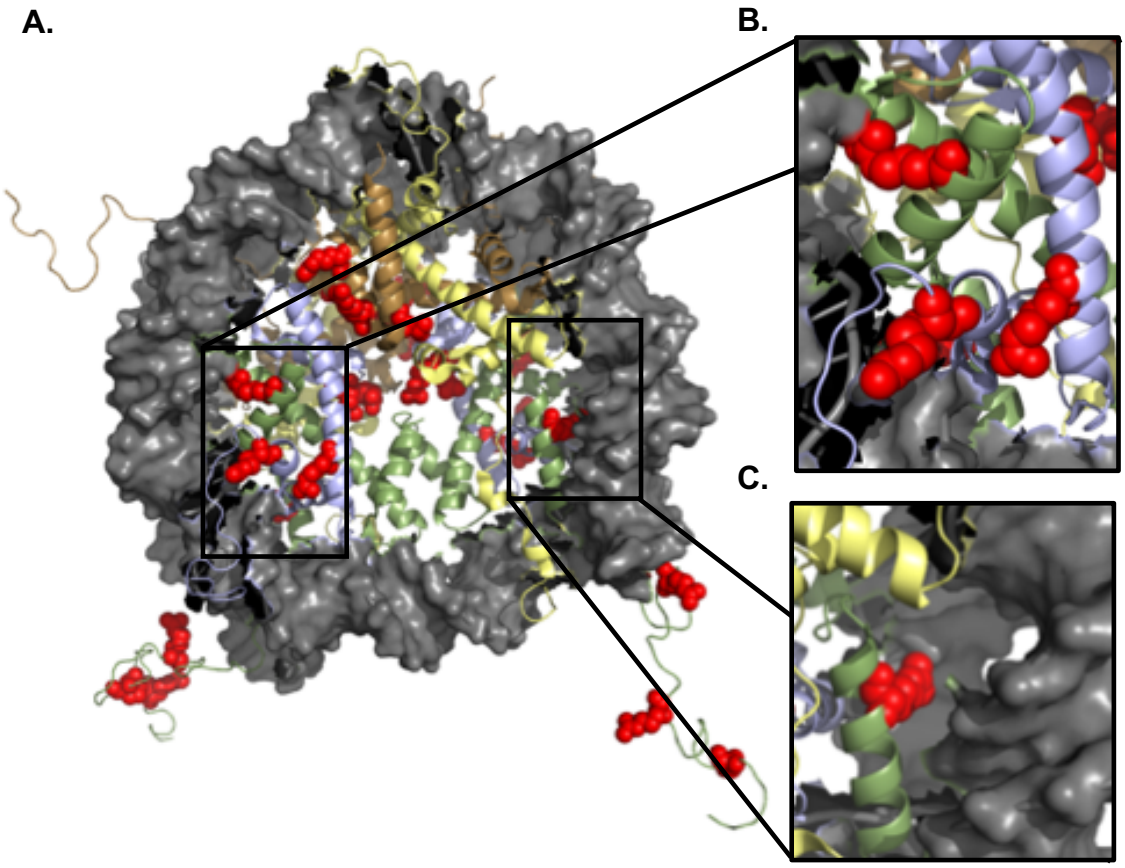

Fig. S9. (*A*) Mapping identified sites of modification (red) on the nucleosome core particle. (*B, C*) H4R23, H4R55, and H3R72 all lie within close proximity to DNA. PDB: 1KX5.

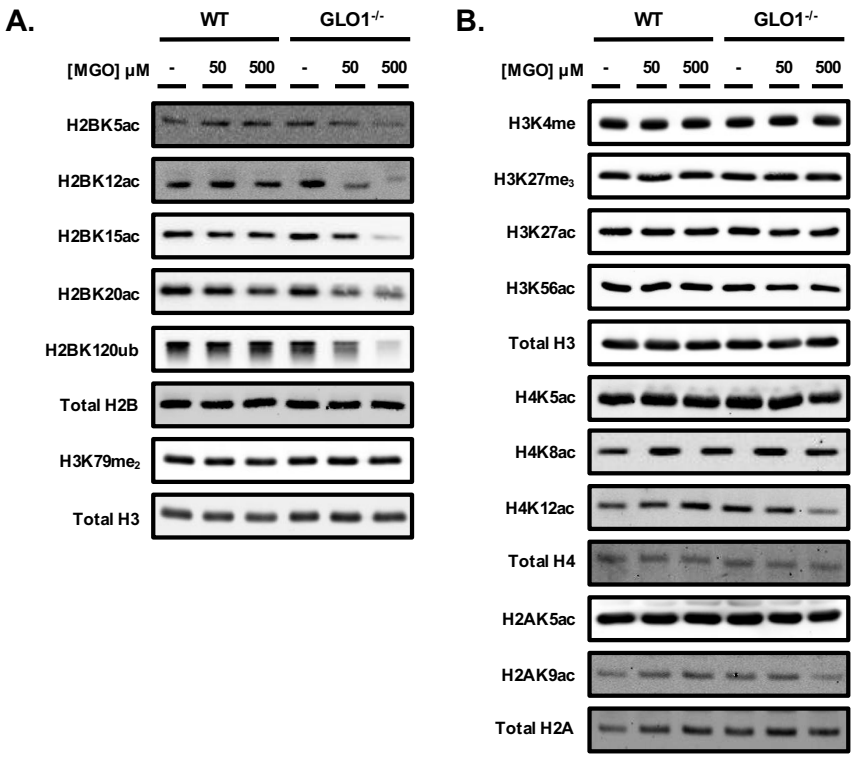

Fig. S10. WT or GLO1$^{-/-}$ cells were treated with 50 or 500 μM MGO for 6 h, and chromatin was extracted and subjected to immunoblotting. (*A*) MGO leads to a marked disruption in H2B acetylation and ubiquitylation, while preserving H3K79me$_2$. (*B*) No alterations in H2A, H3, or H4 PTMs were observed. Shown are representative blots from a single N = 3 experiment.

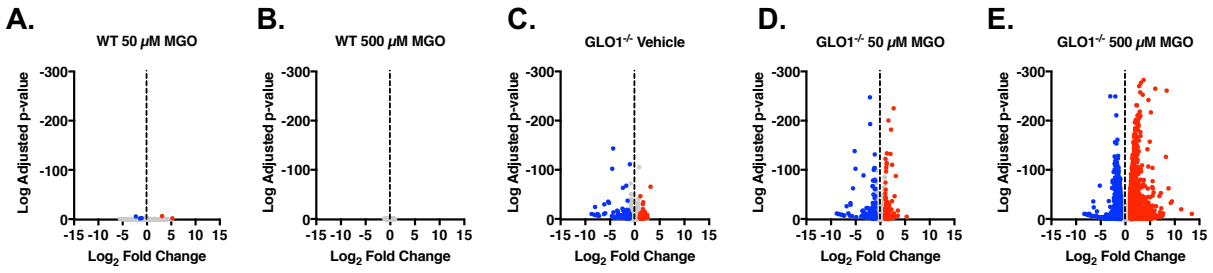

Fig. S11. RNA-Seq reveals transcripts altered by MGO. *(A-E)* Volcano plots reveal all RNA significantly increased (red) or decreased (blue) compared to WT vehicle control (Log_2 fold change > 2, $P < 0.05$). N = 3 for each cohort.

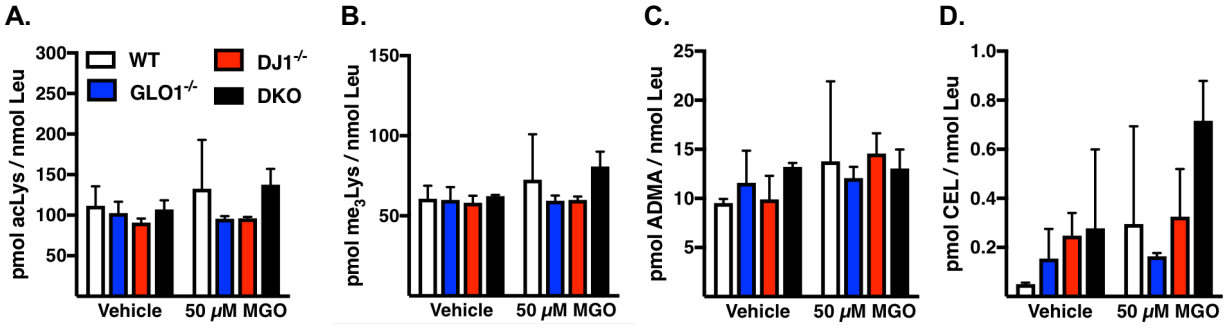

Fig. S12. QuARKMod was performed on chromatin fractions isolated from each cohort, demonstrating no changes in (*A*) acLys, (*B*) me$_3$Lys, (*C*) ADMA, or (*D*) CEL. Treatments were for 6 h. Data are presented as the mean ± S.D., N = 3, and statistical significance was determined via two-way ANOVA (*** $p < 0.001$).

MS/MS spectra of identified MG-H, CEA, or CEL adducts.

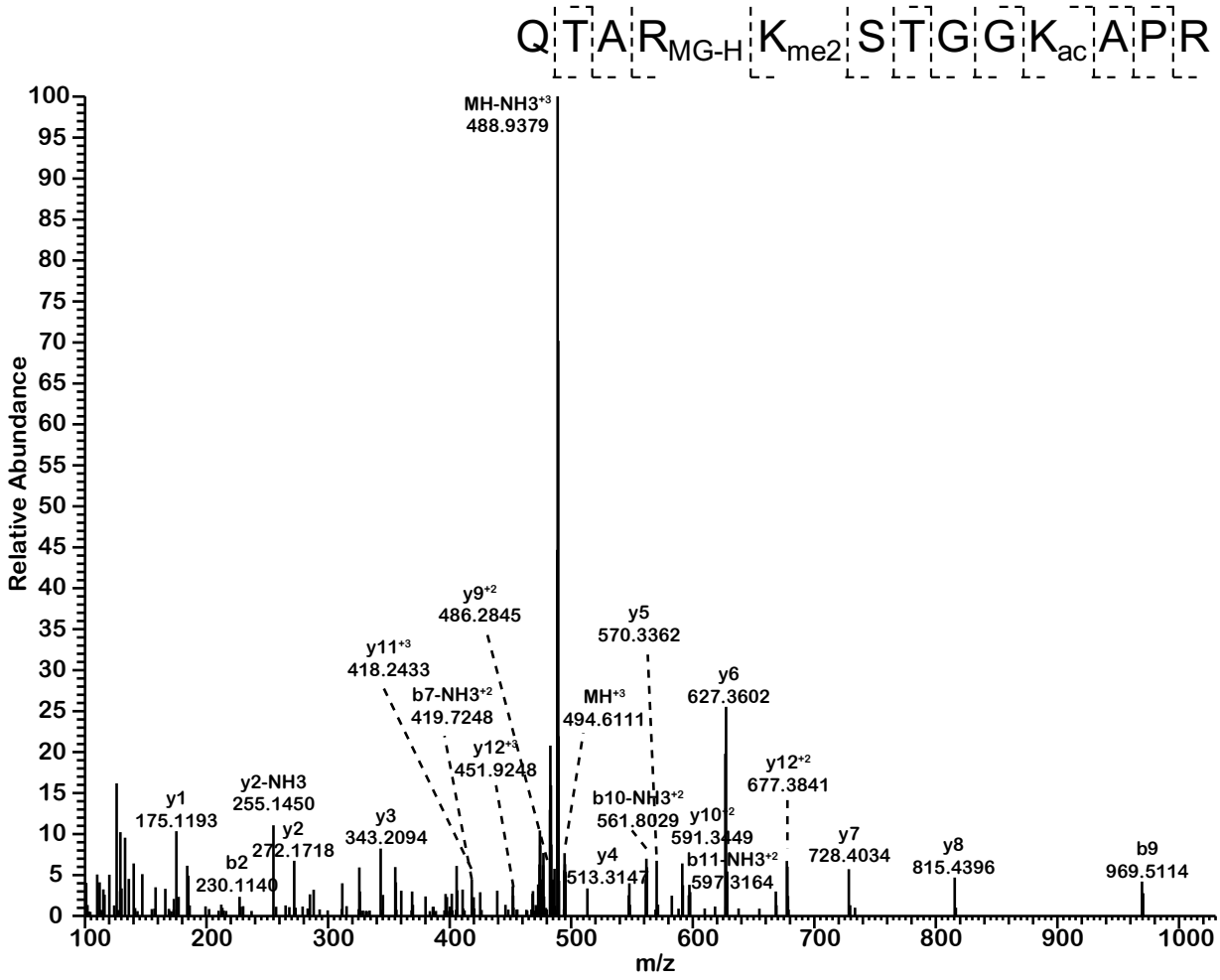

Fig. S13. MS/MS spectra of the MG-H adduct identified at H3R8; Δ 2.02 ppm, retention time of 51.62 min.

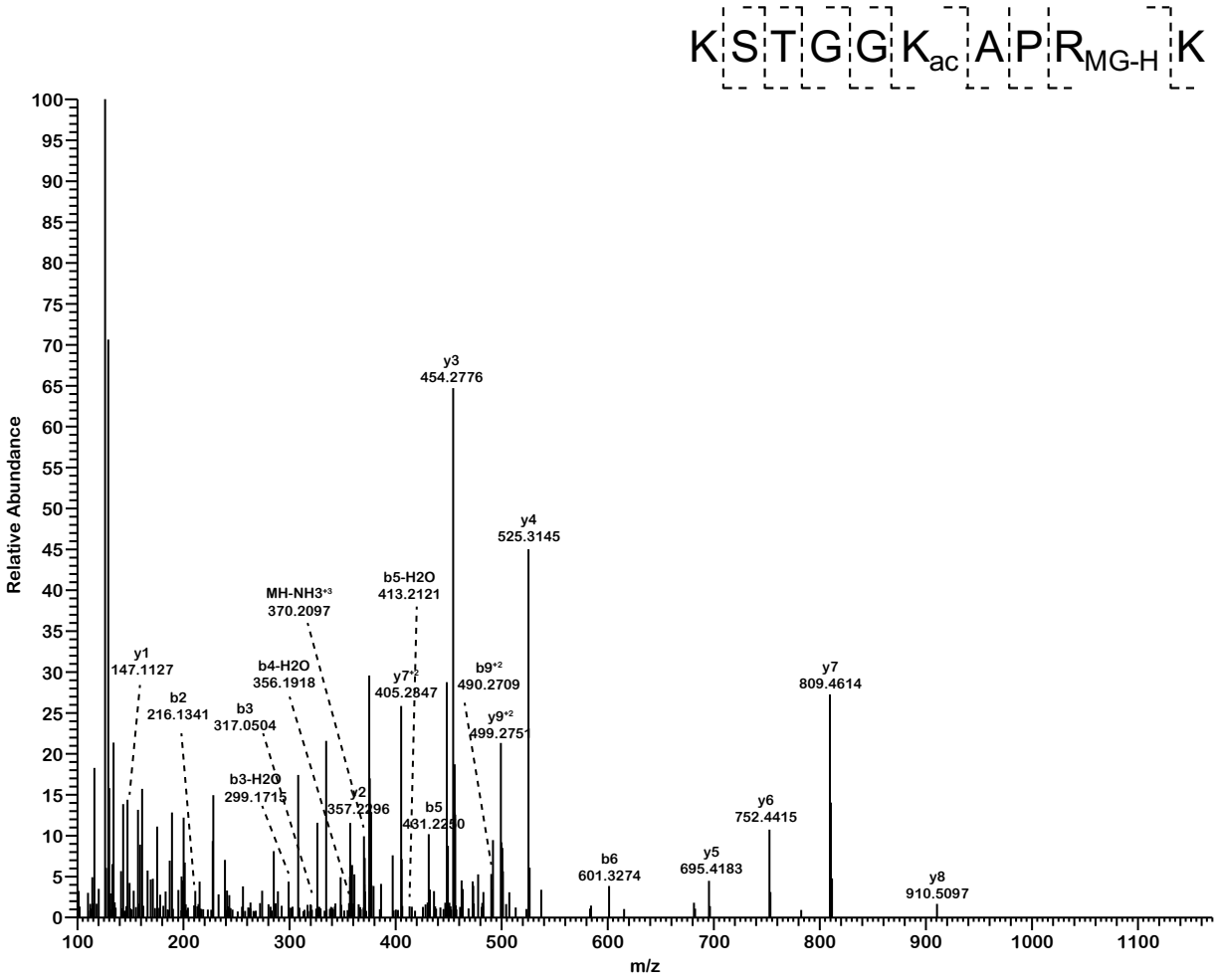

Fig. S14. MS/MS spectra of the MG-H adduct identified at H3R19; Δ 10.9 ppm, retention time of 11.29 min.

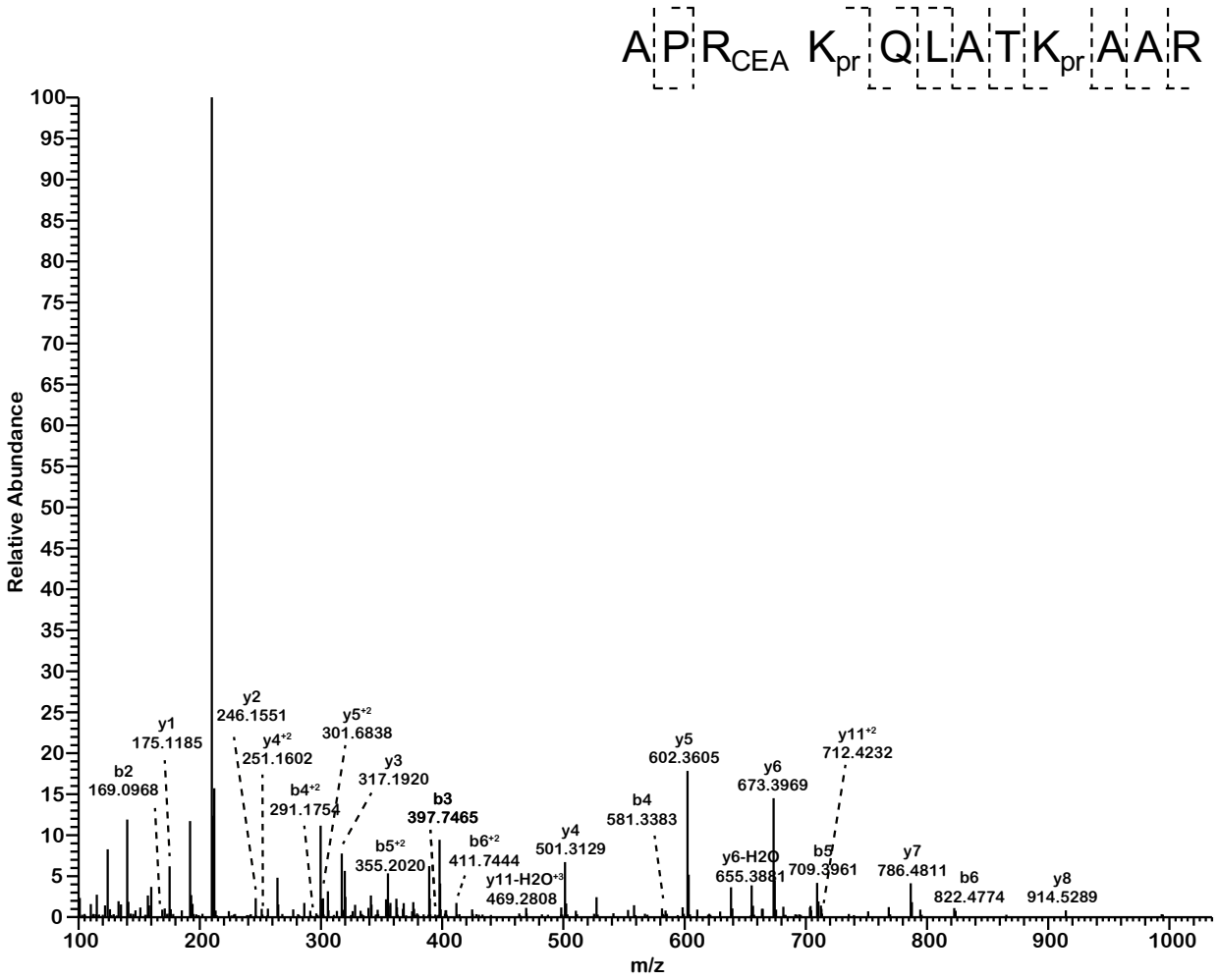

Fig. S15. MS/MS spectra of the CEA adduct identified at H3R19; Δ 2.4 ppm, retention time of 28.51 min.

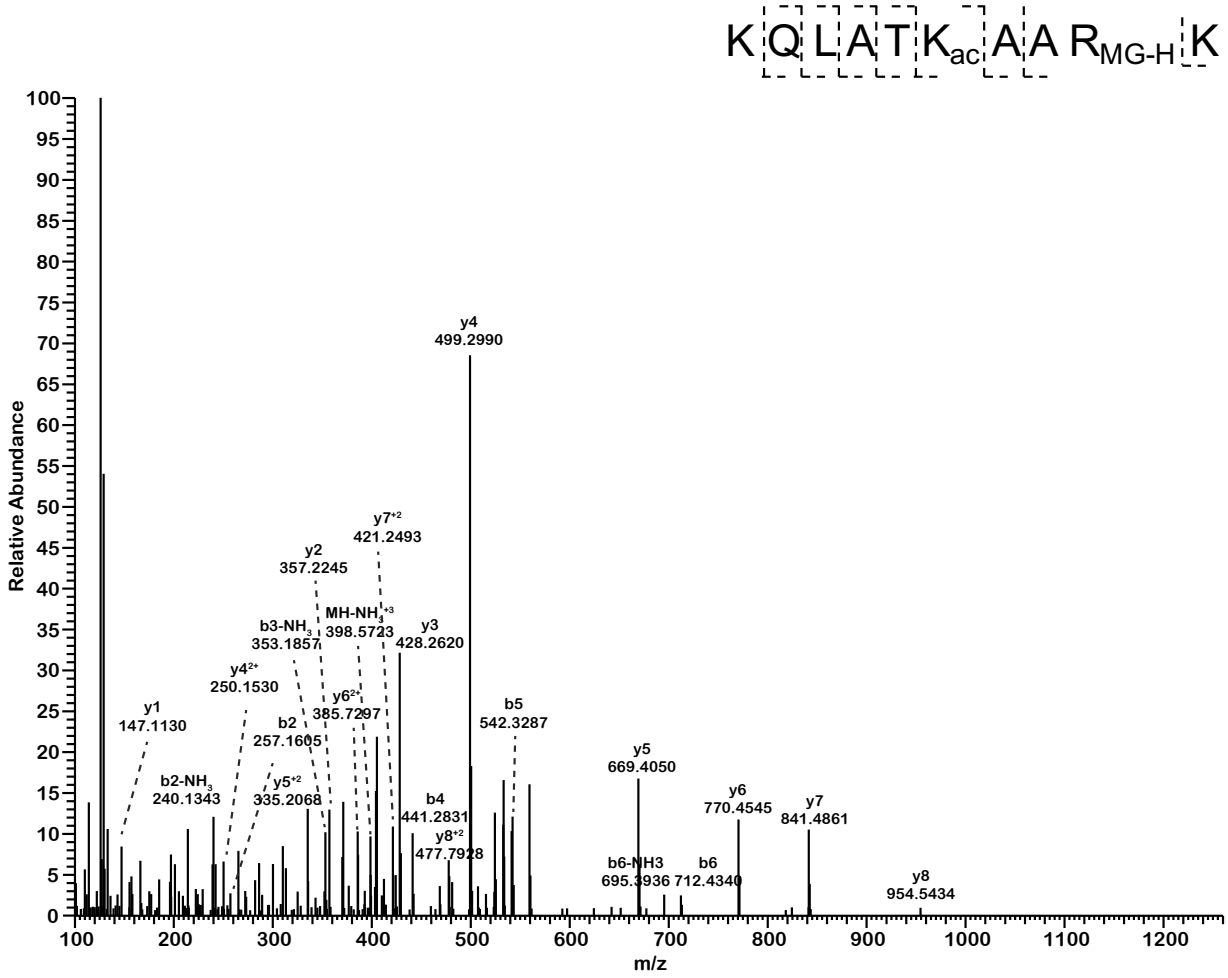

Fig. S16. MS/MS spectra of the MG-H adduct identified at H3R26; Δ 0.25 ppm, retention time of 51.98 min.

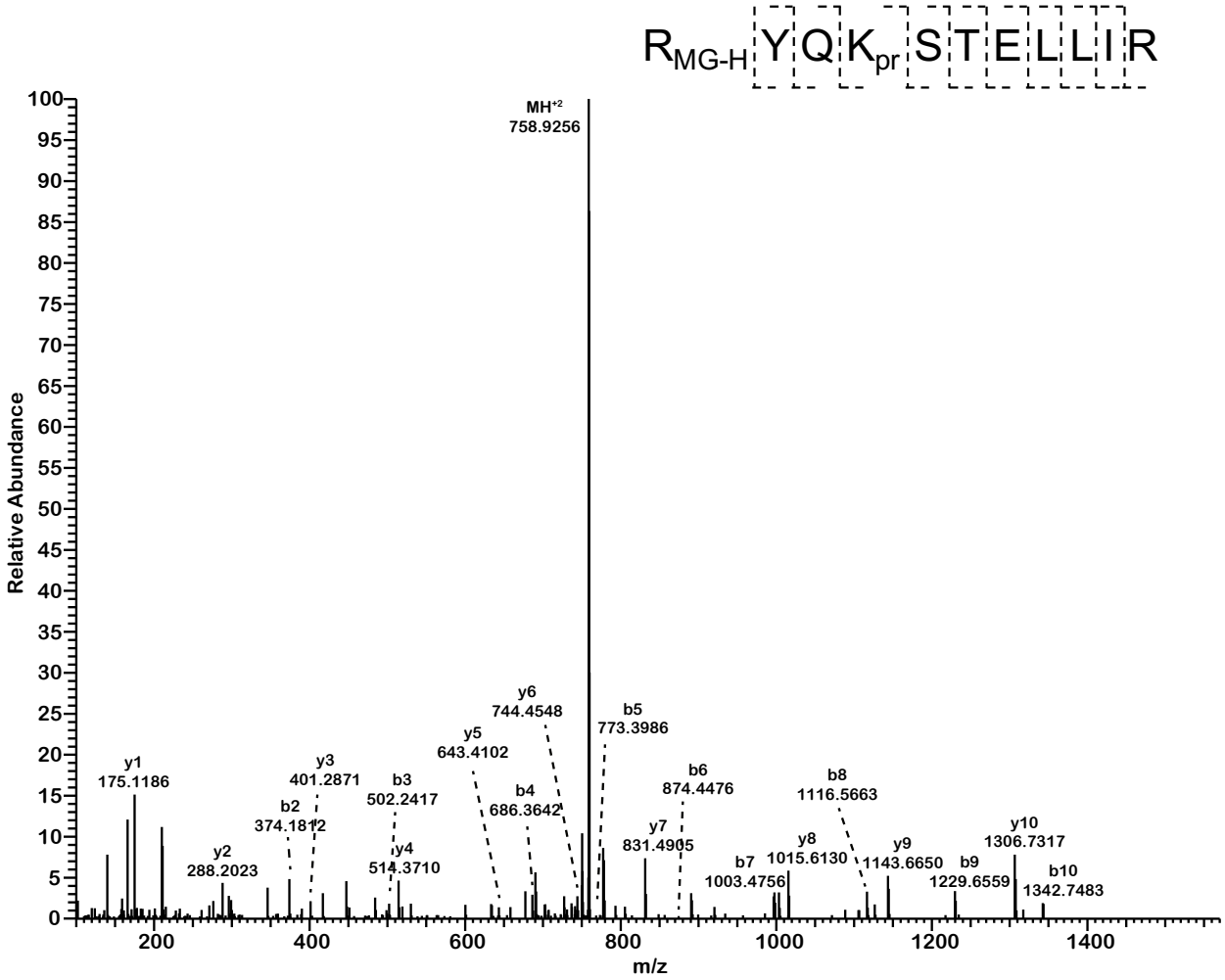

Fig. S17. MS/MS spectra of the MG-H adduct identified at H3R53; Δ 6.32 ppm, retention time of 45.12 min.

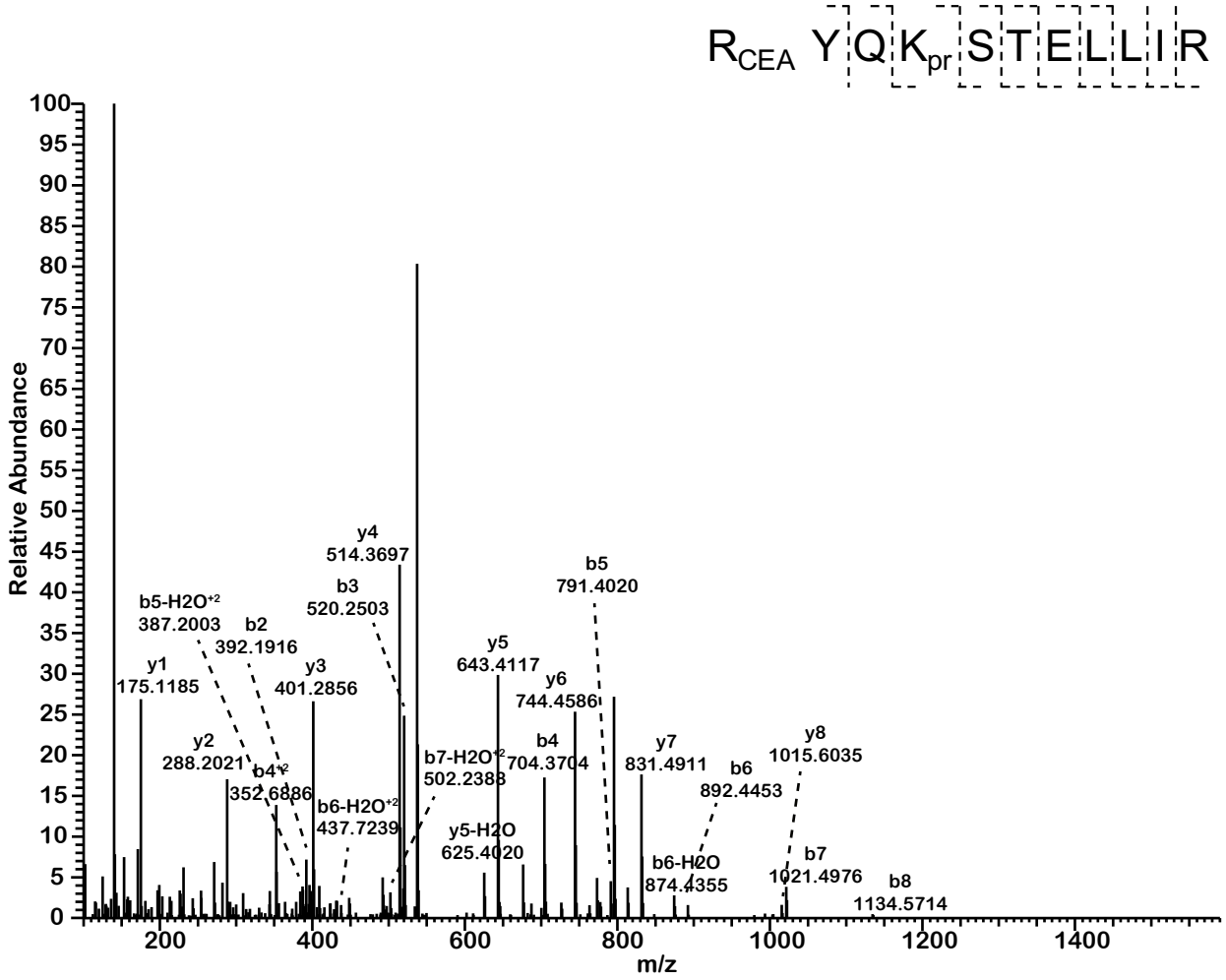

Fig. S18. MS/MS spectra of the CEA adduct identified at H3R53; Δ 2.14 ppm, retention time of 43.95 min.

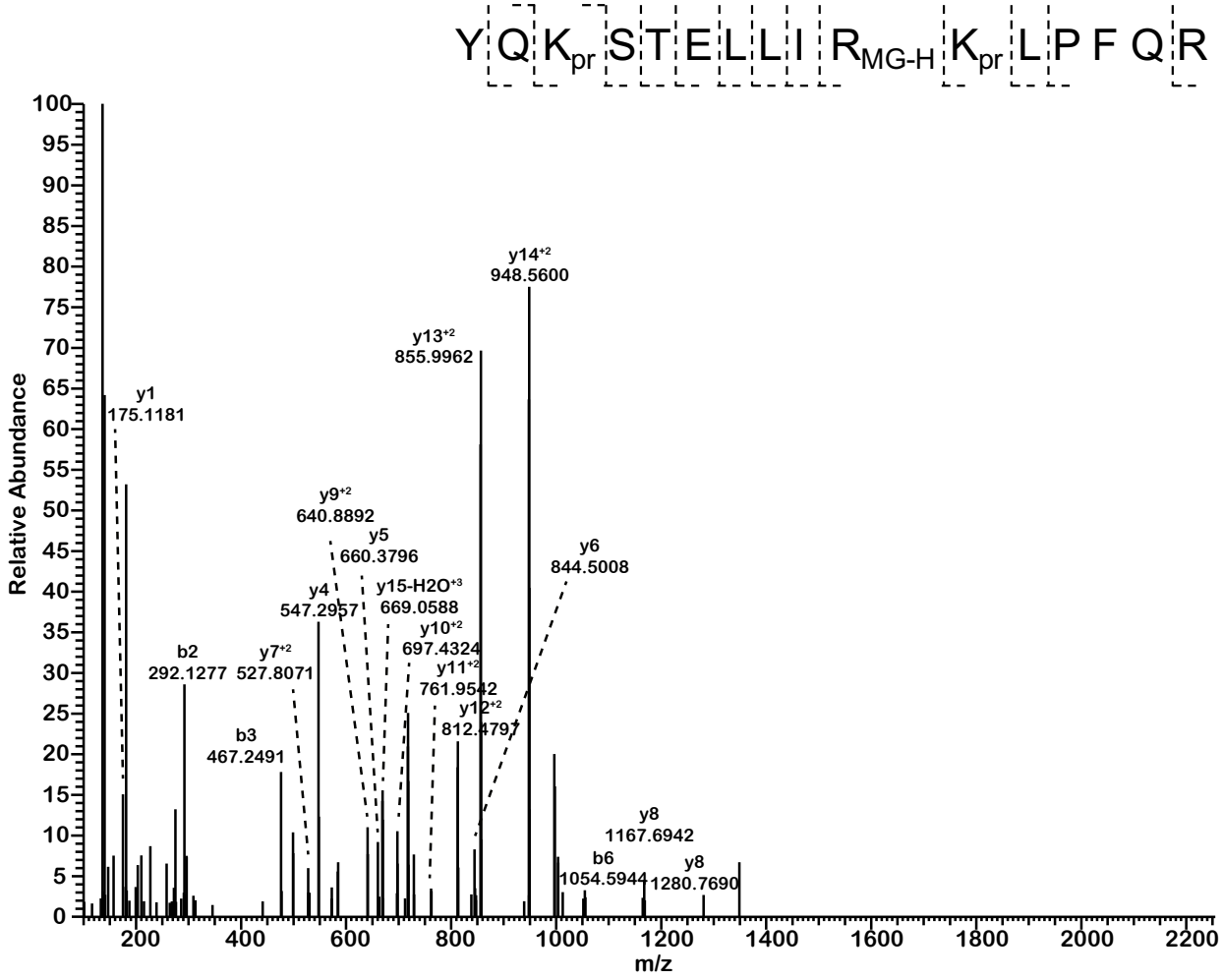

Fig. S19. MS/MS spectra of the MG-H adduct identified at H3R63; Δ 1.37 ppm, retention time of 53.99 min.

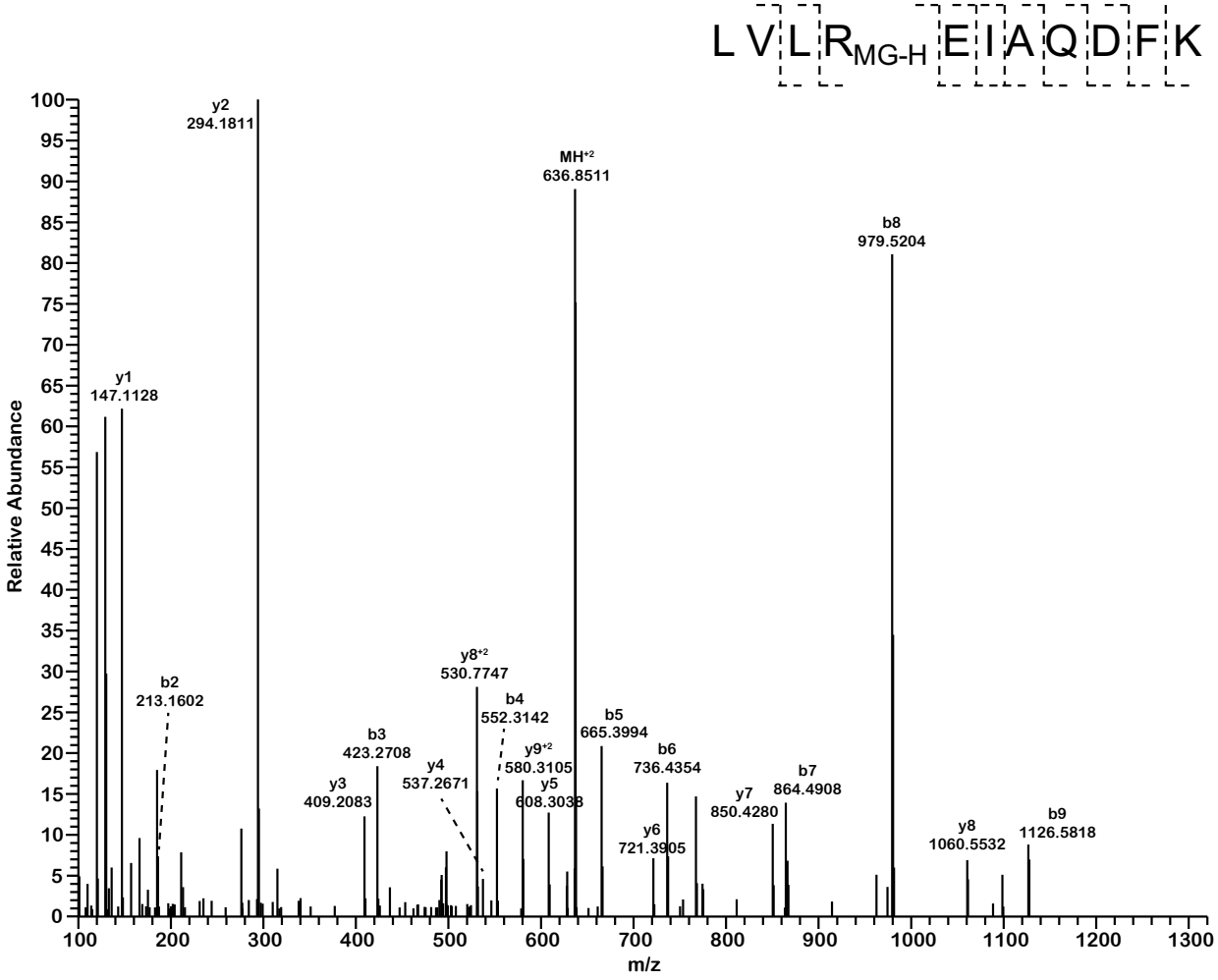

Fig. S20. MS/MS spectra of the MG-H adduct identified at H3R72; Δ 0.16 ppm, retention time of 50.32 min.

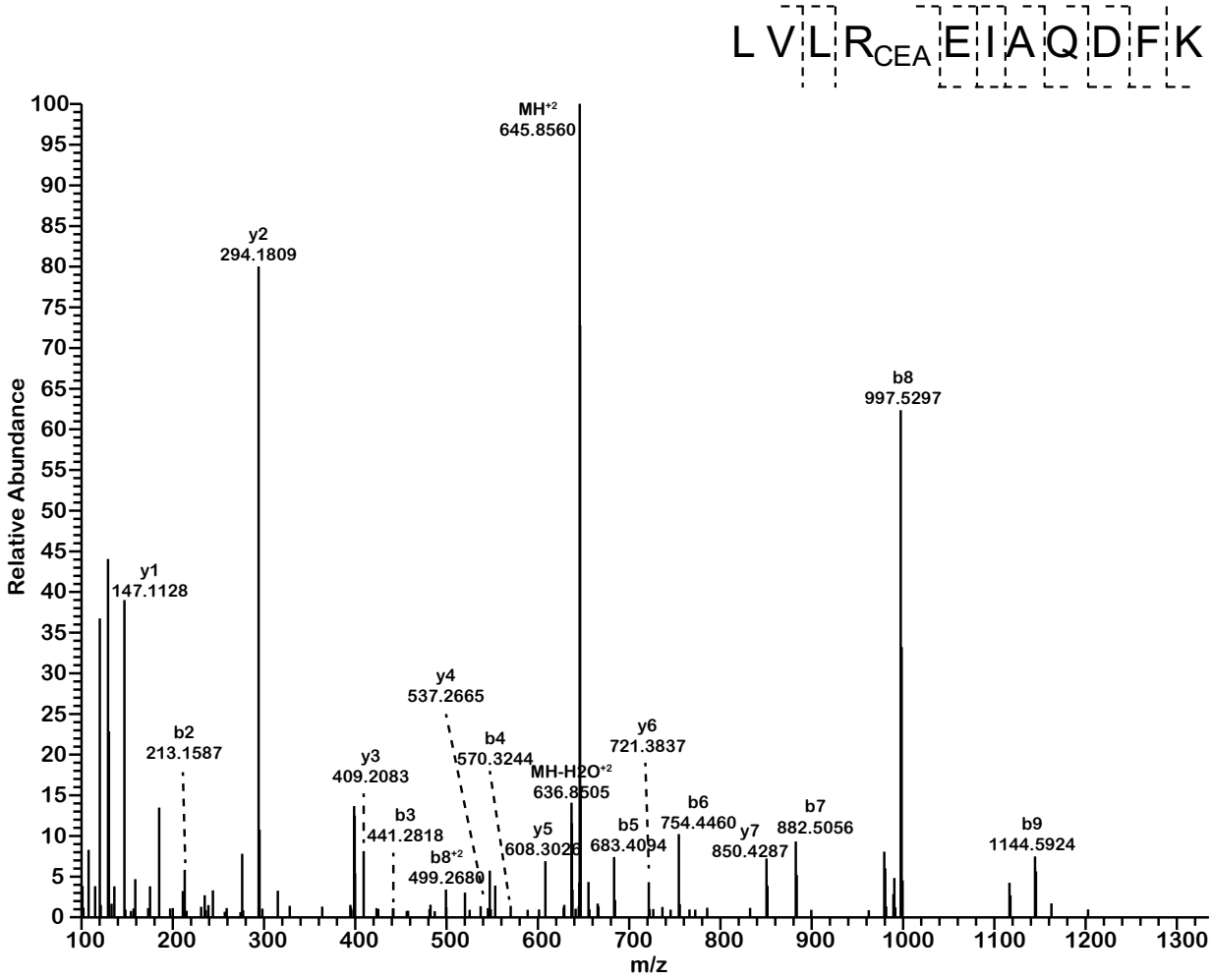

Fig. S21. MS/MS spectra of the CEA adduct identified at H3R72; Δ 0.31 ppm, retention time of 49.22 min.

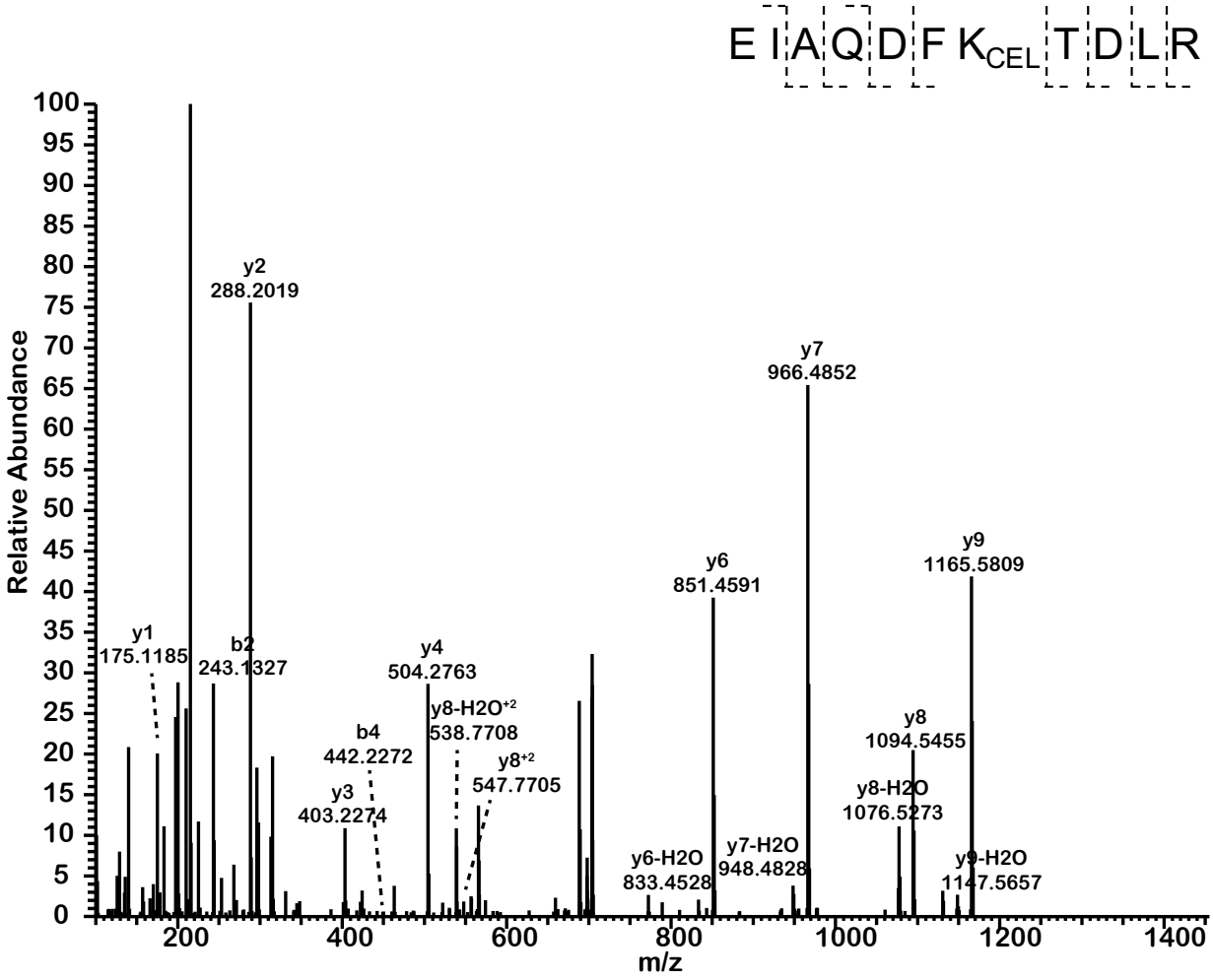

Fig. S22. MS/MS spectra of the CEL adduct identified at H3K79; Δ 1.28 ppm, retention time of 35.08 min.

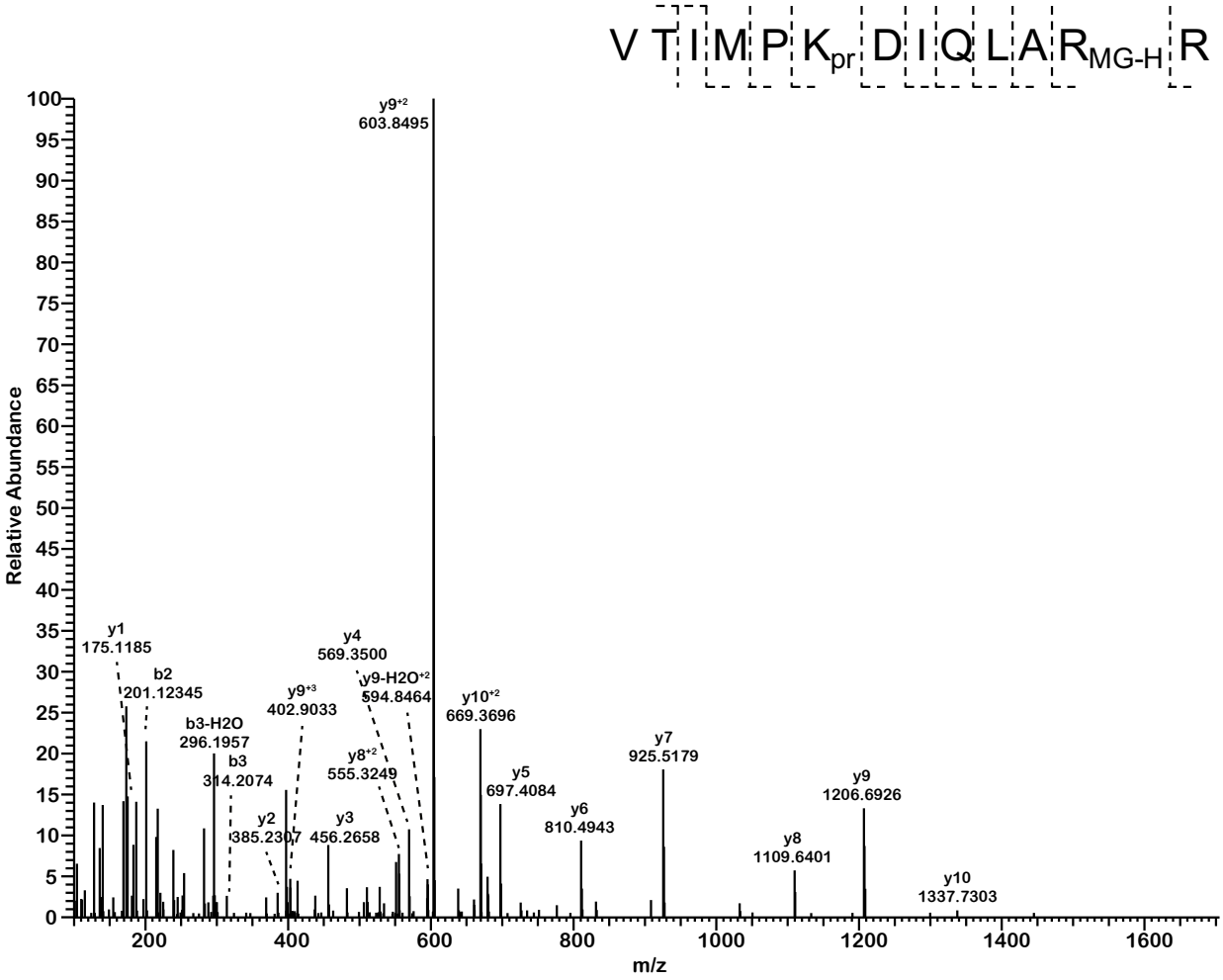

Fig. S23. MS/MS spectra of the MG-H adduct identified at H3R128; Δ 2.17 ppm, retention time of 45.73 min.

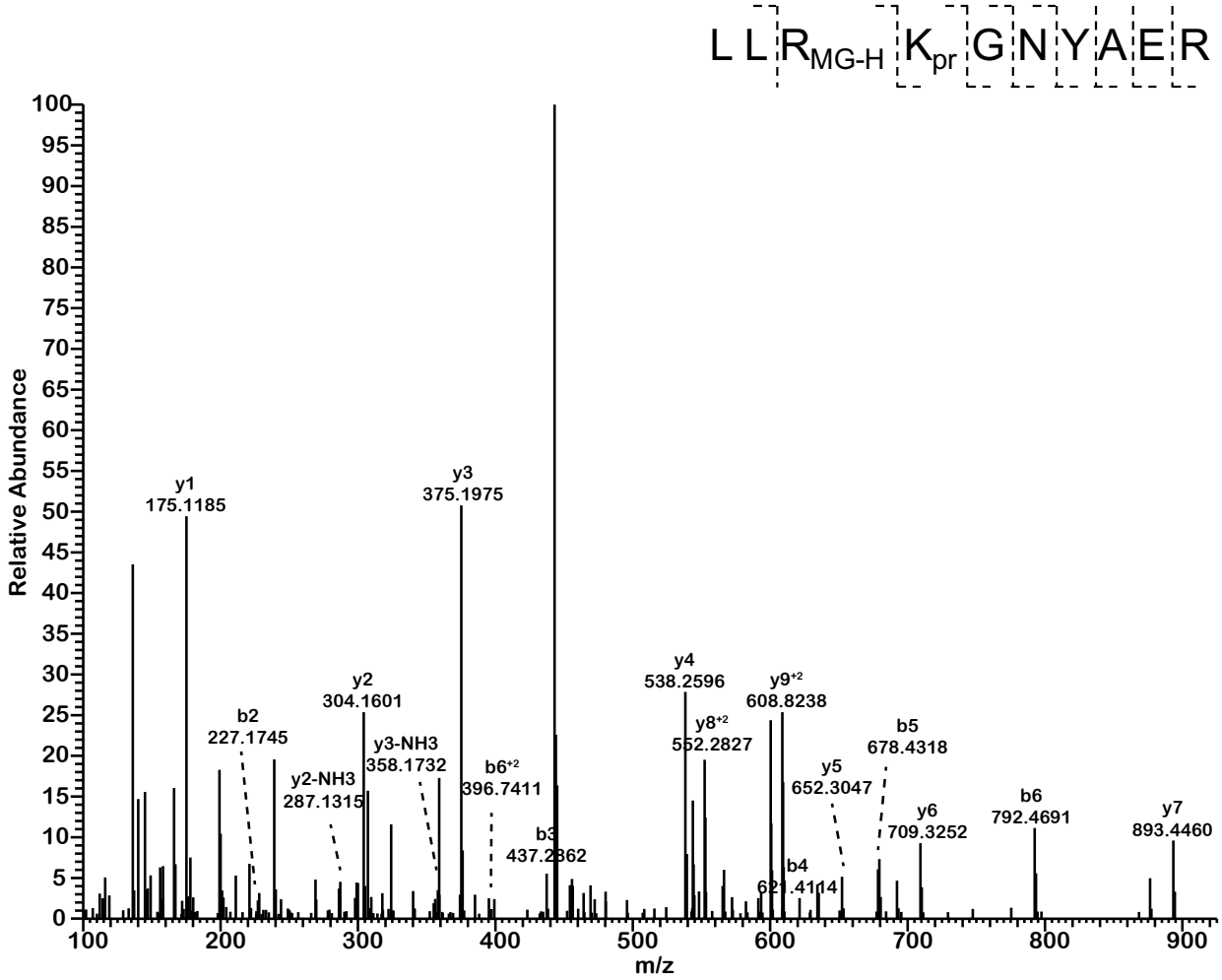

Fig. S24. MS/MS spectra of the MG-H adduct identified at H2AR35; Δ 4.05 ppm, retention time of 39.18 min.

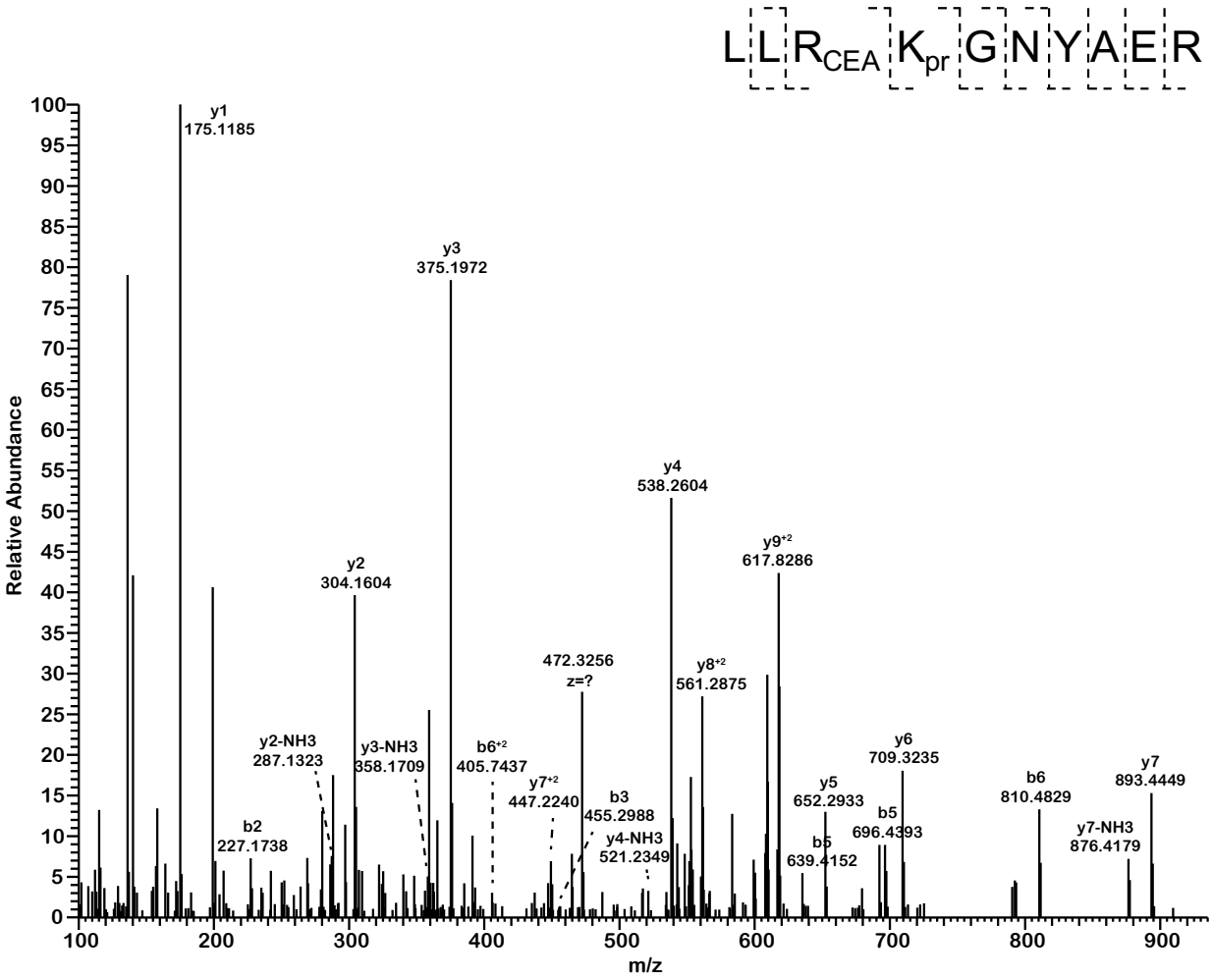

Fig. S25. MS/MS spectra of the CEA adduct identified at H2AR35; Δ 3.55 ppm, retention time of 38.62 min.

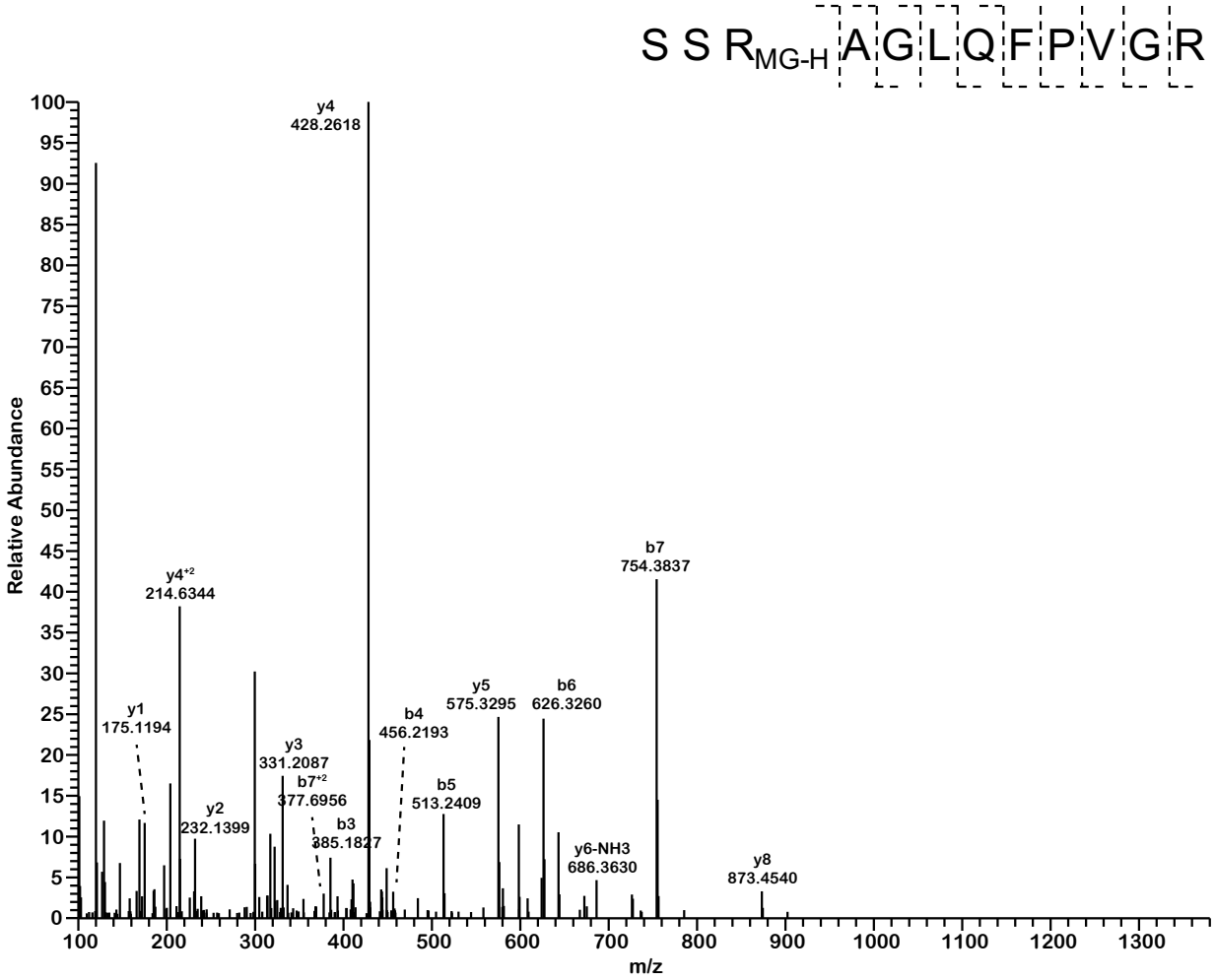

Fig. S26. MS/MS spectra of the MG-H adduct identified at H2AxR20; Δ 0.90 ppm, retention time of 46.54 min.

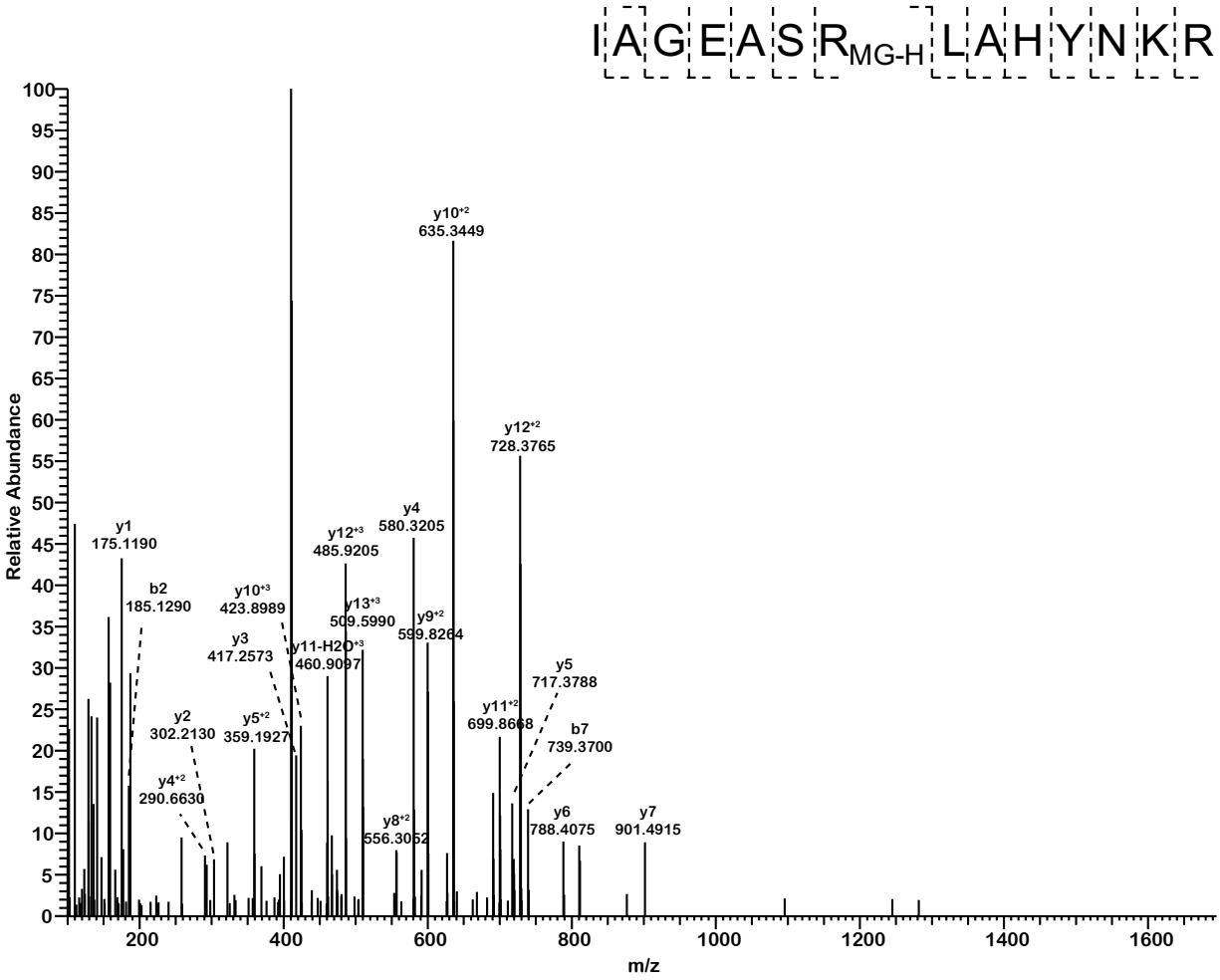

Fig. S27. MS/MS spectra of the MG-H adduct identified at H2BR79; Δ -0.48 ppm, retention time of 57.12 min.

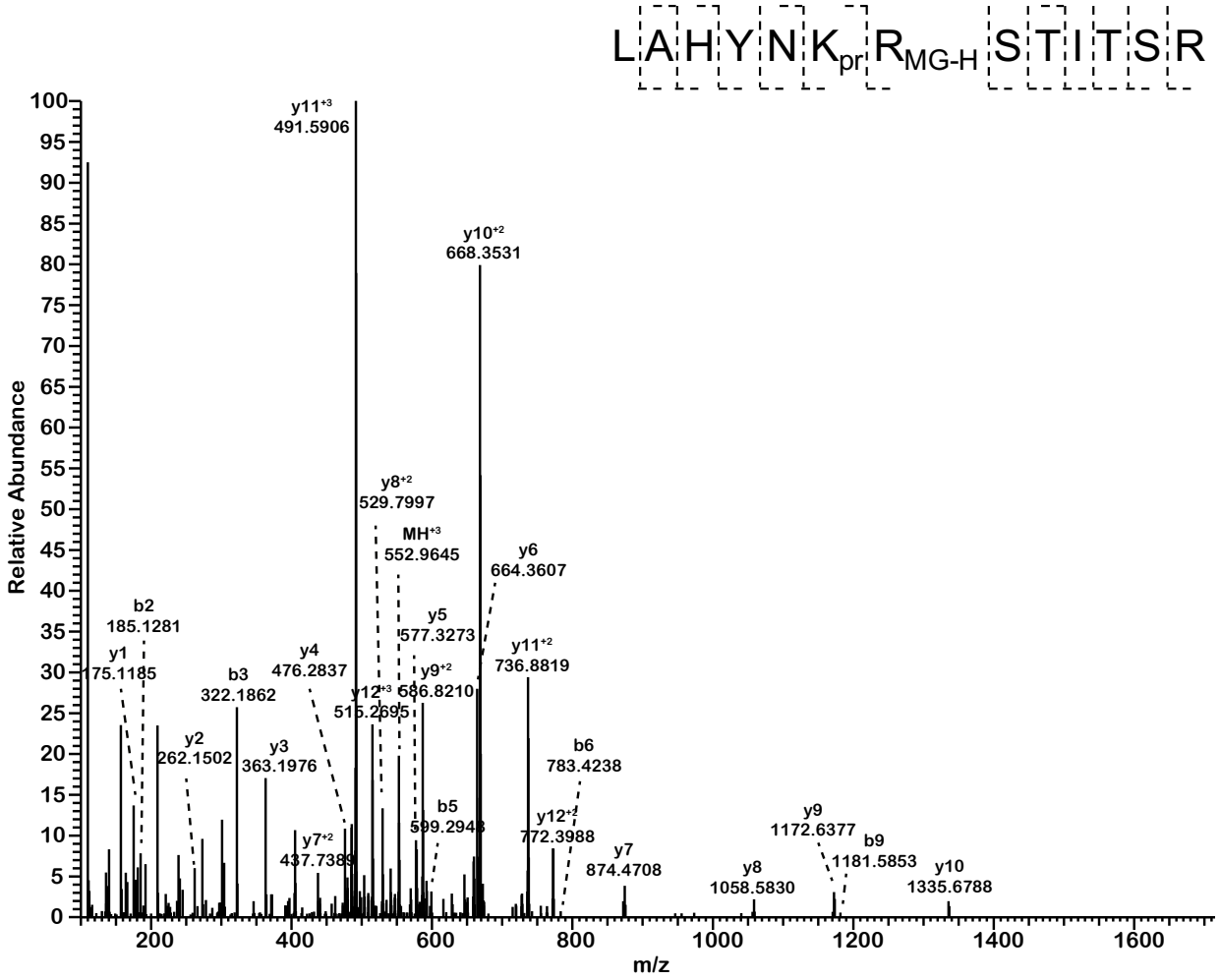

Fig. S28. MS/MS spectra of the MG-H adduct identified at H2BR86; Δ -0.36 ppm, retention time of 25.87 min.

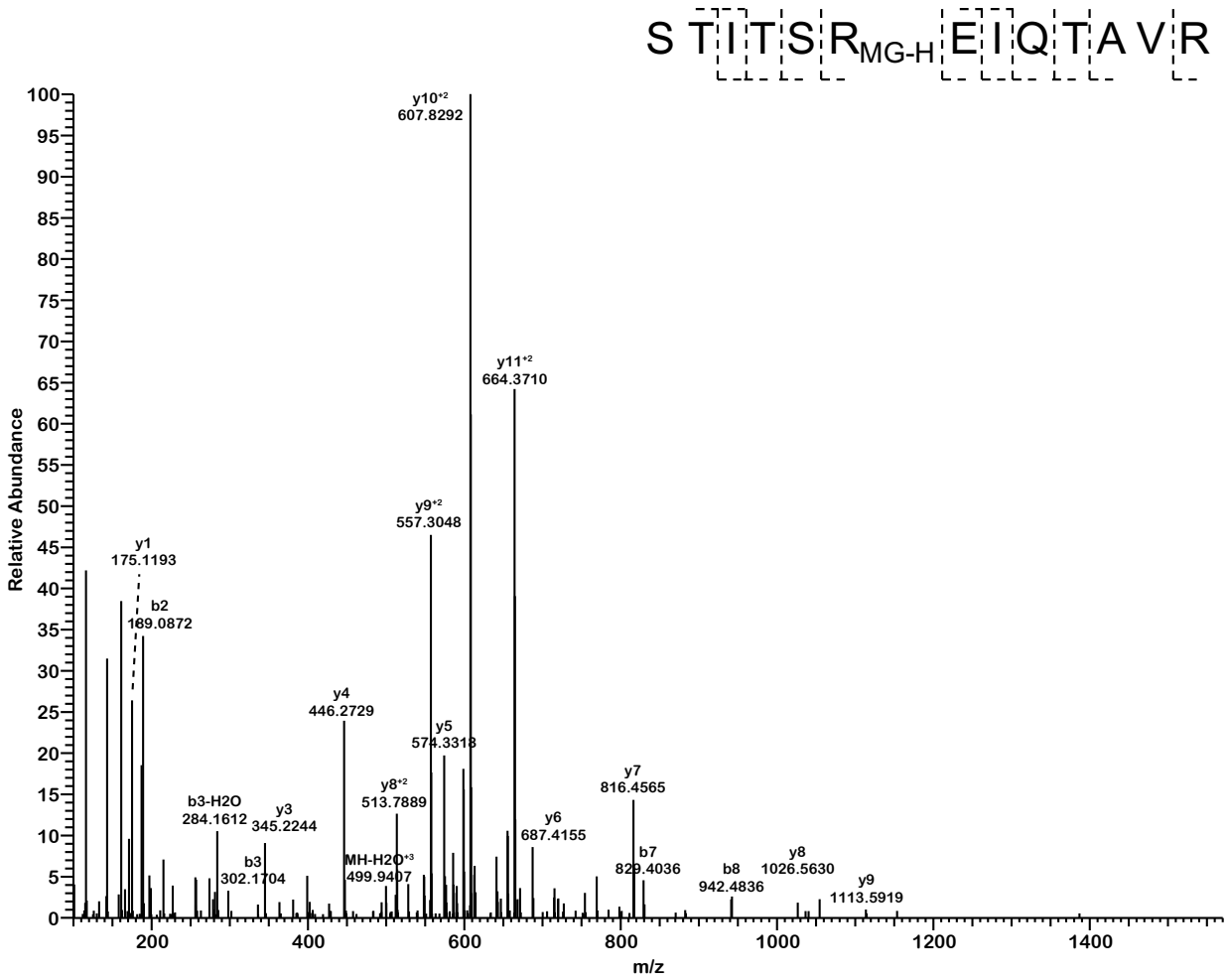

Fig. S29. MS/MS spectra of the MG-H adduct identified at H2BR92; Δ 0.98 ppm, retention time of 49.58 min.

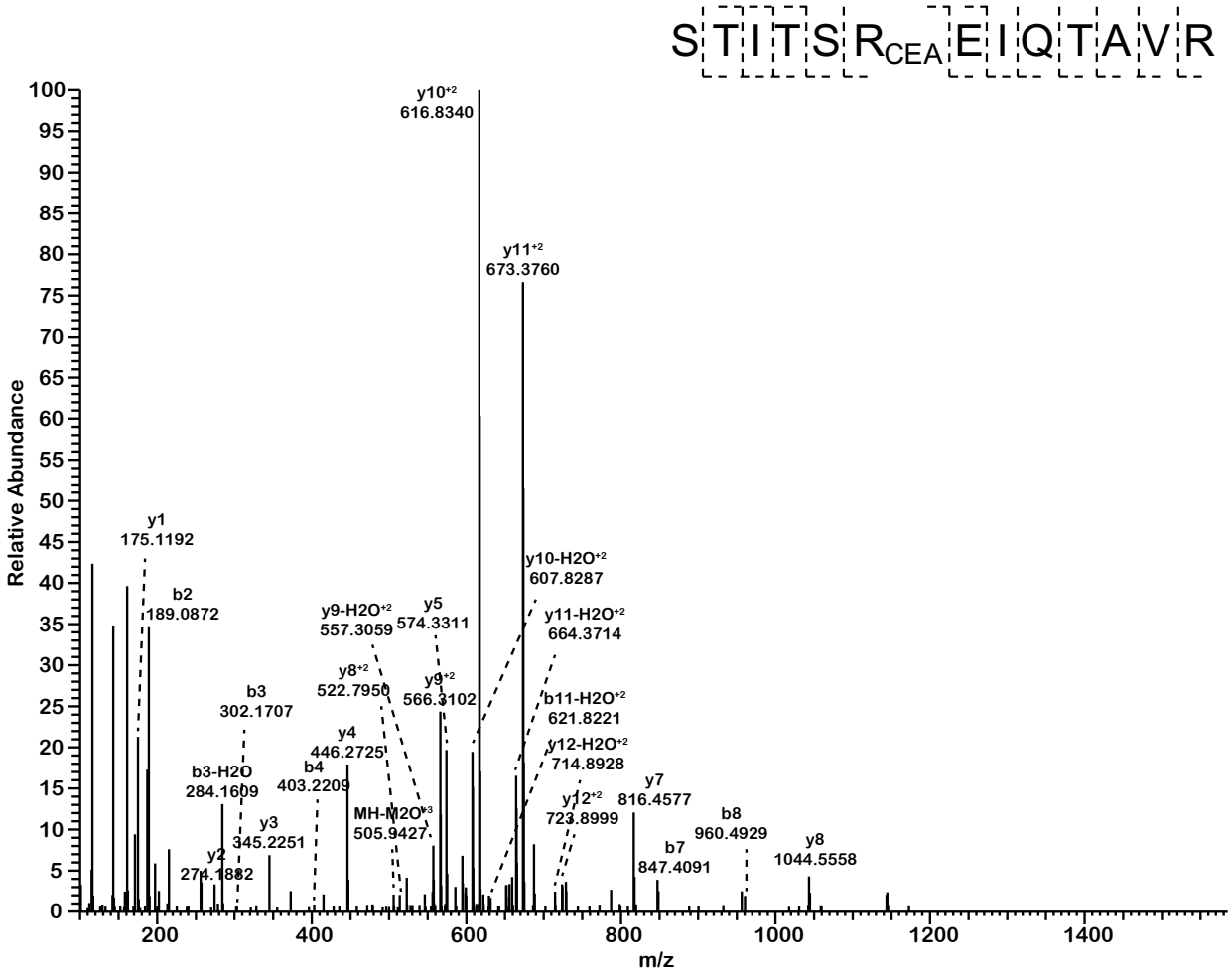

Fig. S30. MS/MS spectra of the CEA adduct identified at H2BR92; Δ -0.19 ppm, retention time of 45.88 min.

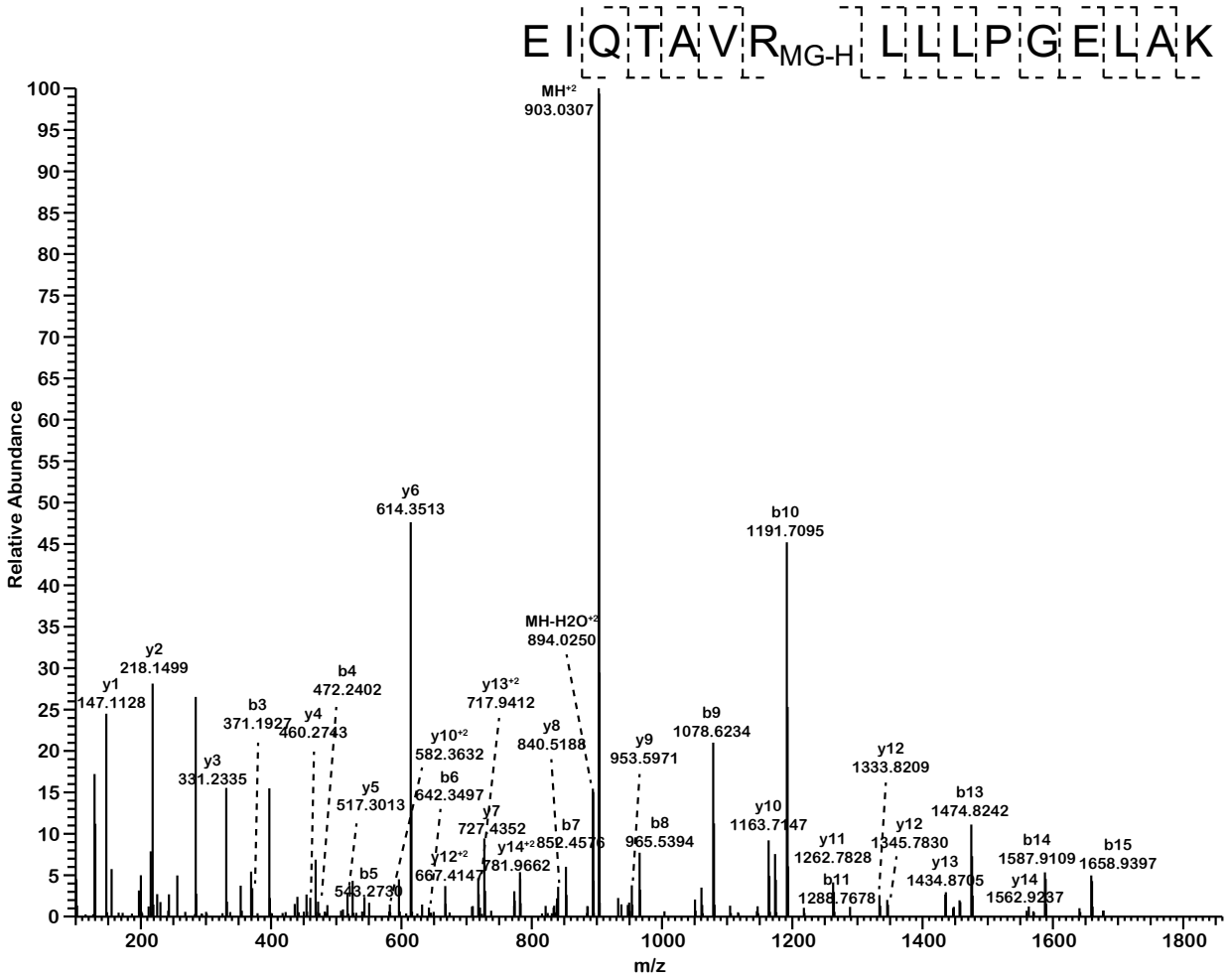

Fig. S31. MS/MS spectra of the MG-H adduct identified at H2BR99; Δ 1.44 ppm, retention time of 60.55 min.

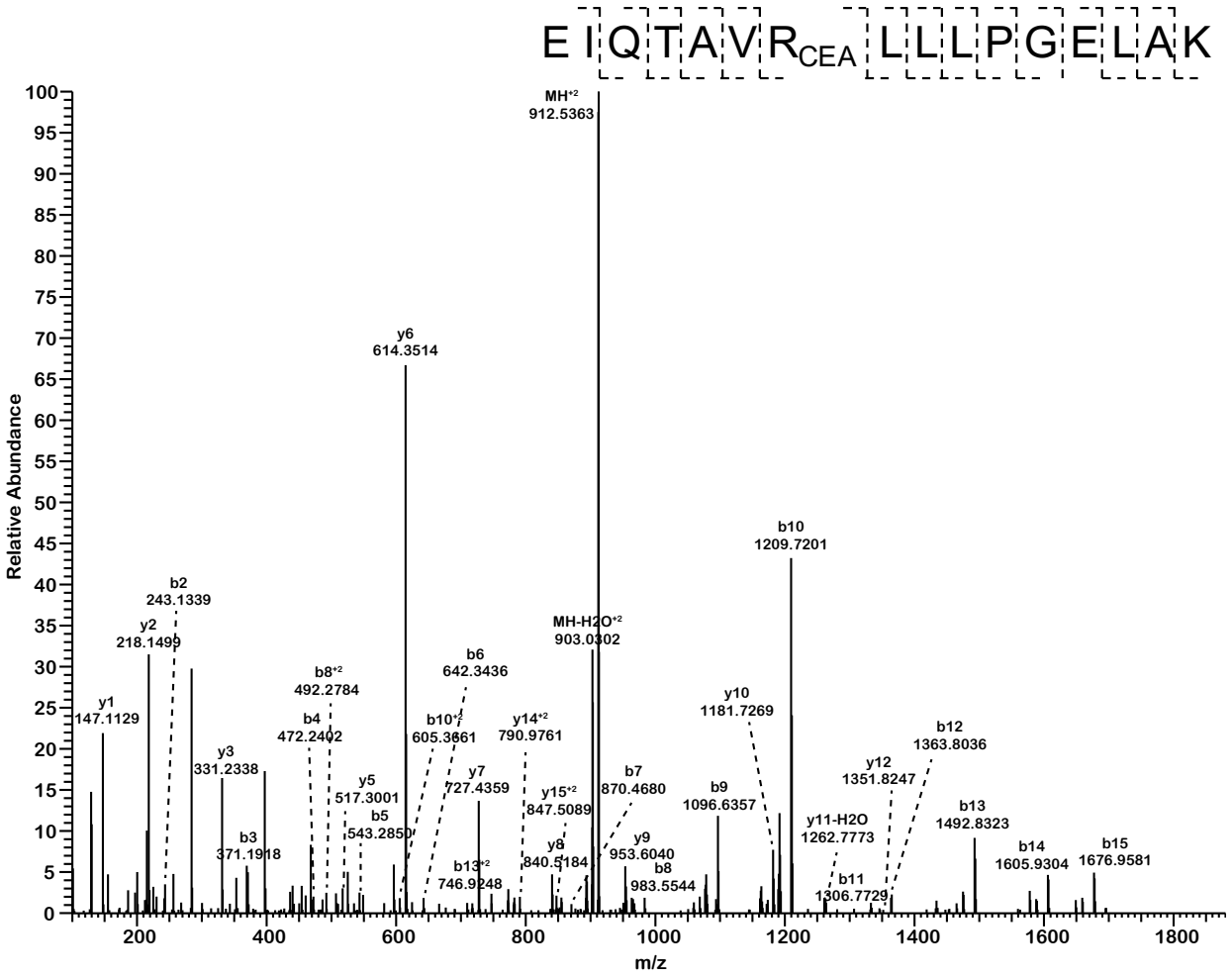

Fig. S32. MS/MS spectra of the CEA adduct identified at H2BR99; Δ 1.09 ppm, retention time of 59.79 min.

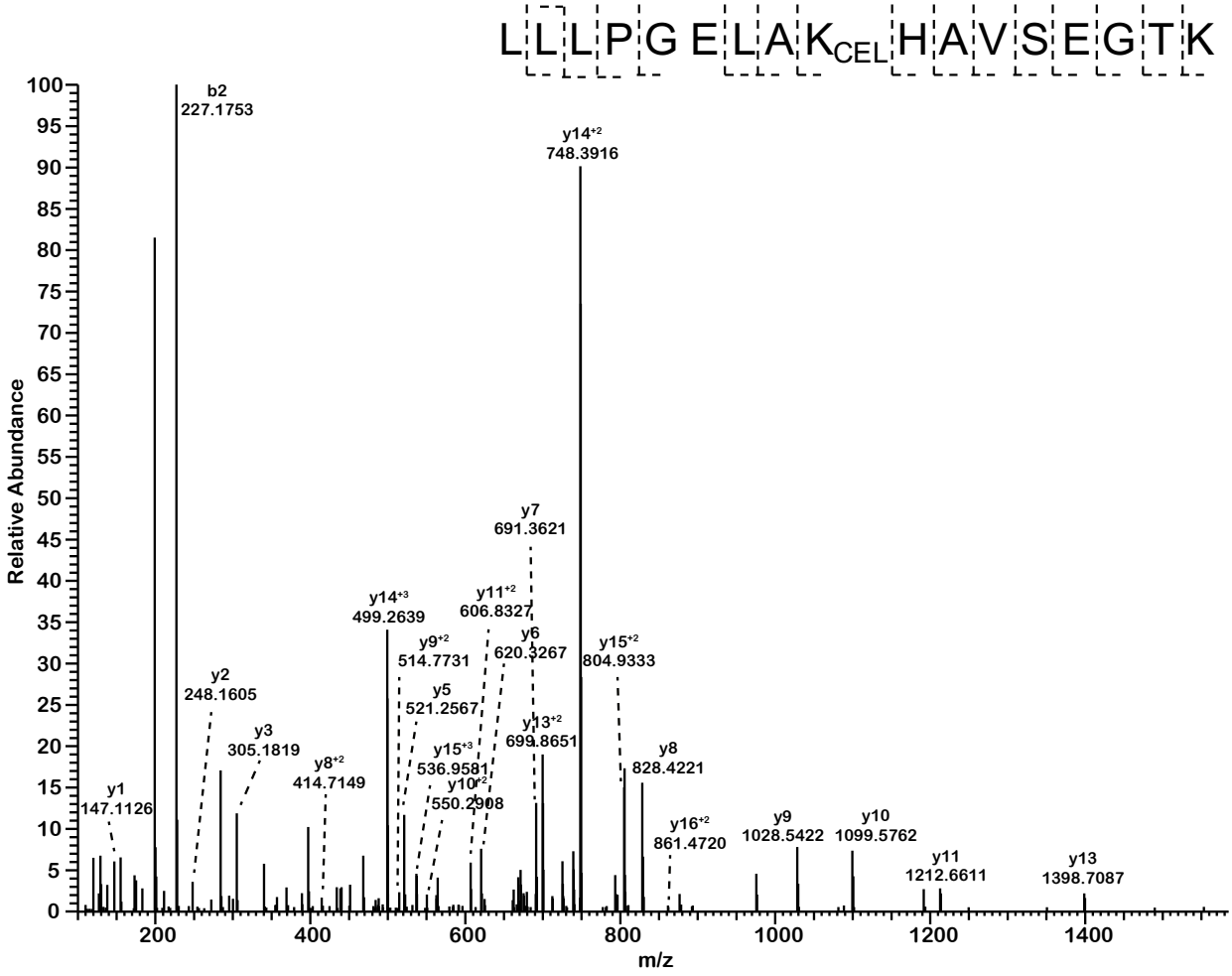

Fig. S33. MS/MS spectra of the CEL adduct identified at H2BK108; Δ 1.46 ppm, retention time of 57.22 min.

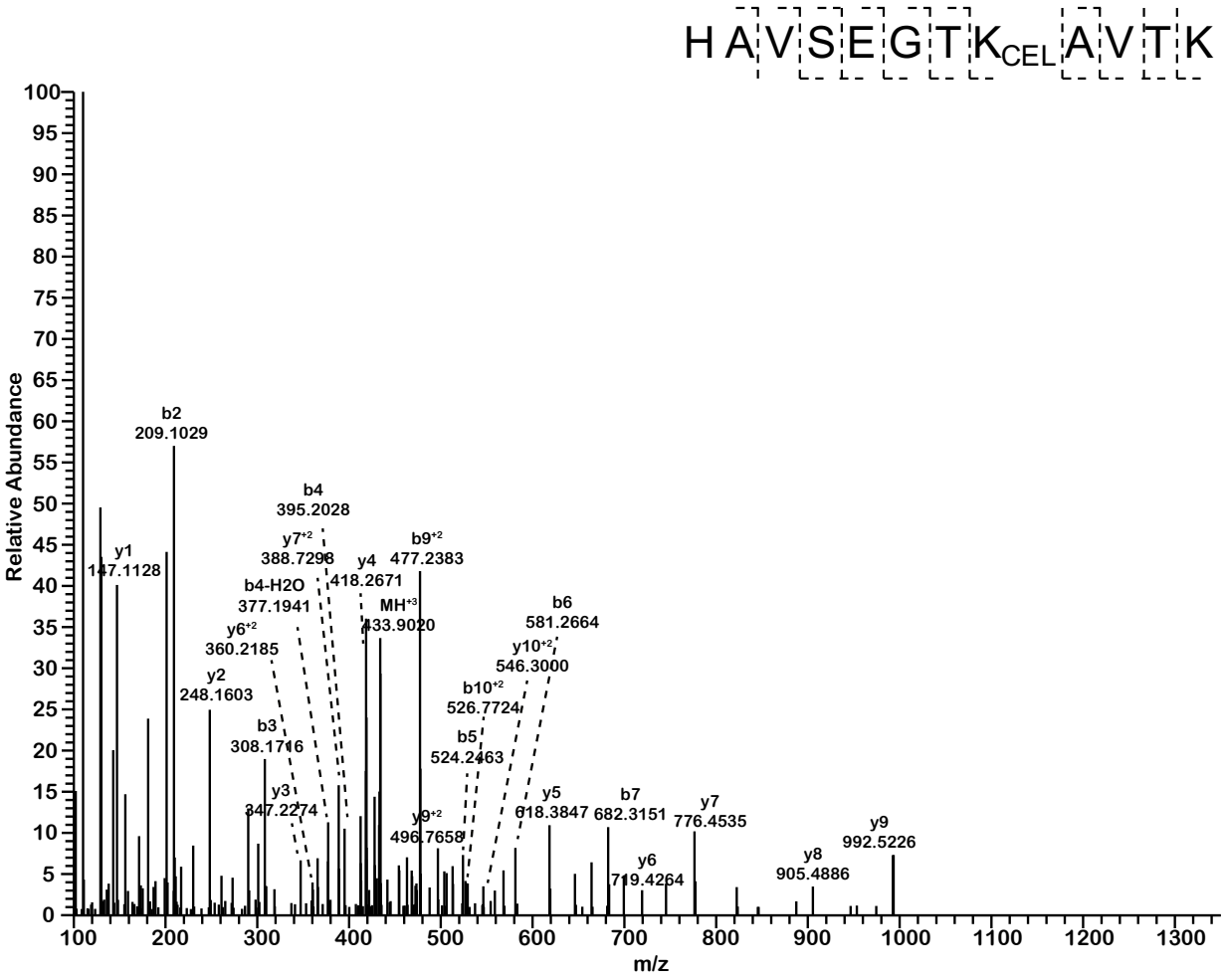

Fig. S34. MS/MS spectra of the CEL adduct identified at H2BK116; Δ -0.23 ppm, retention time of 44.17 min.

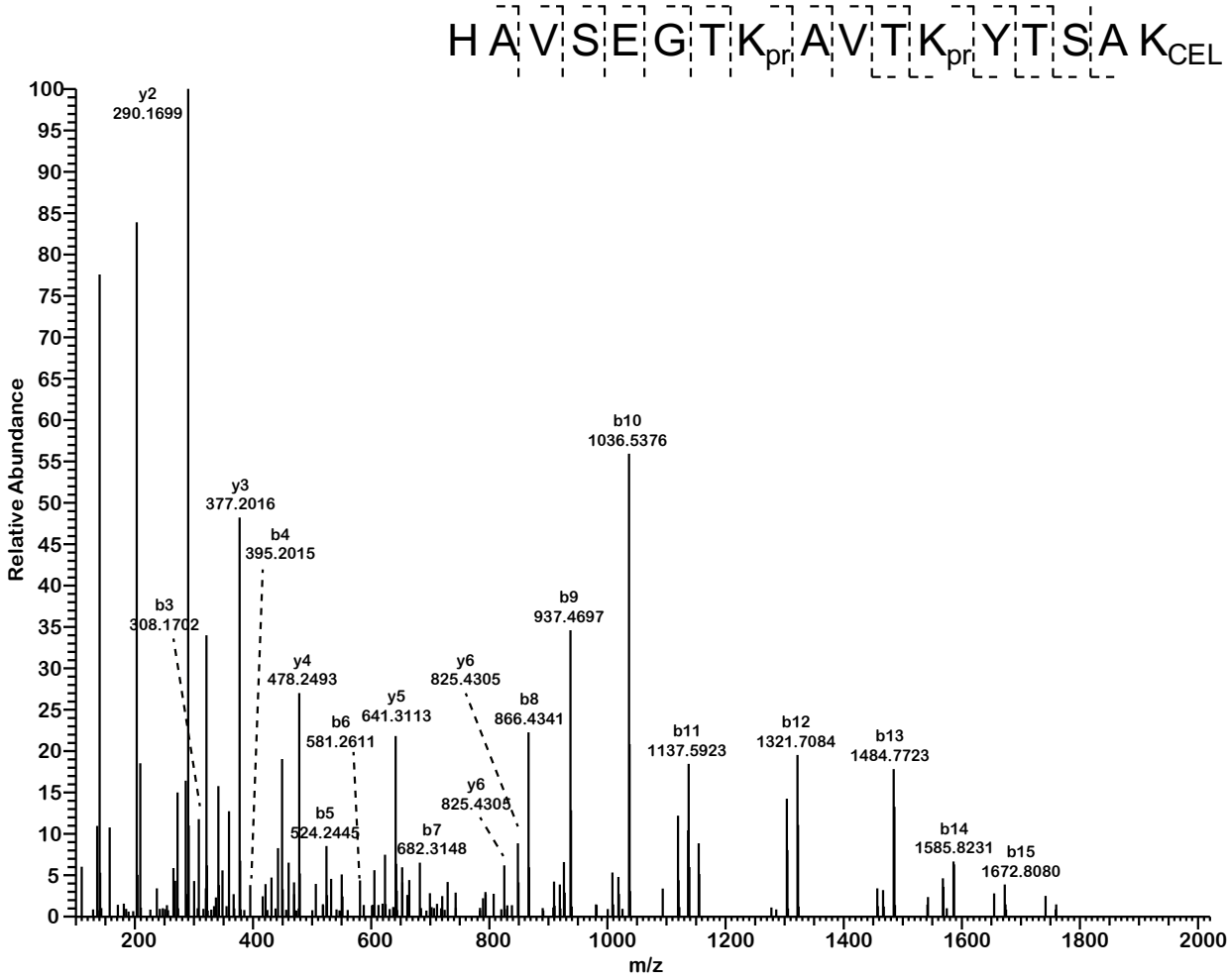

Fig. S35. MS/MS spectra of the CEL adduct identified at H2BK125; Δ 2.34 ppm, retention time of 36.33 min.

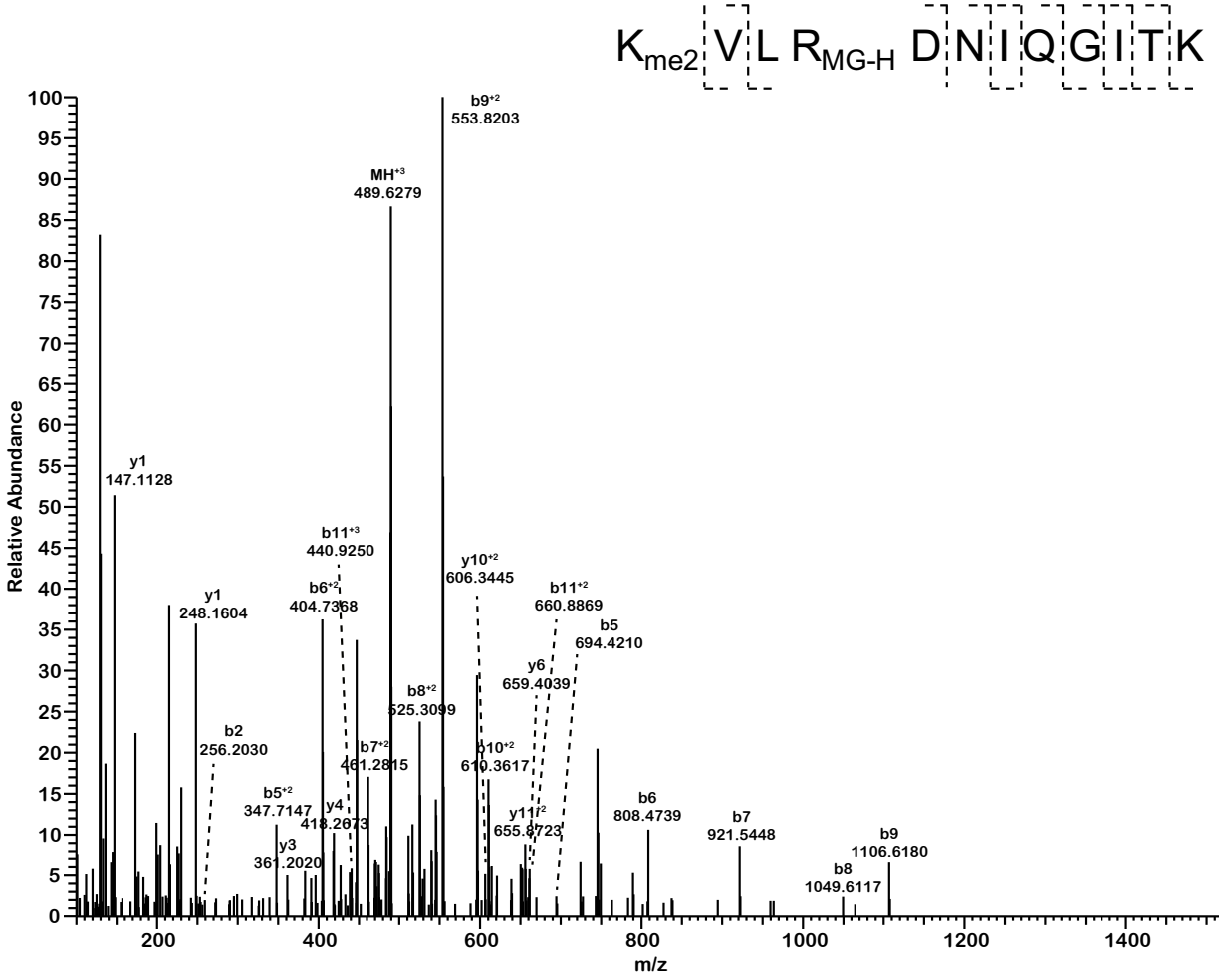

Fig. S36. MS/MS spectra of the MG-H adduct identified at H4R23; Δ 1.22 ppm, retention time of 57.39 min.

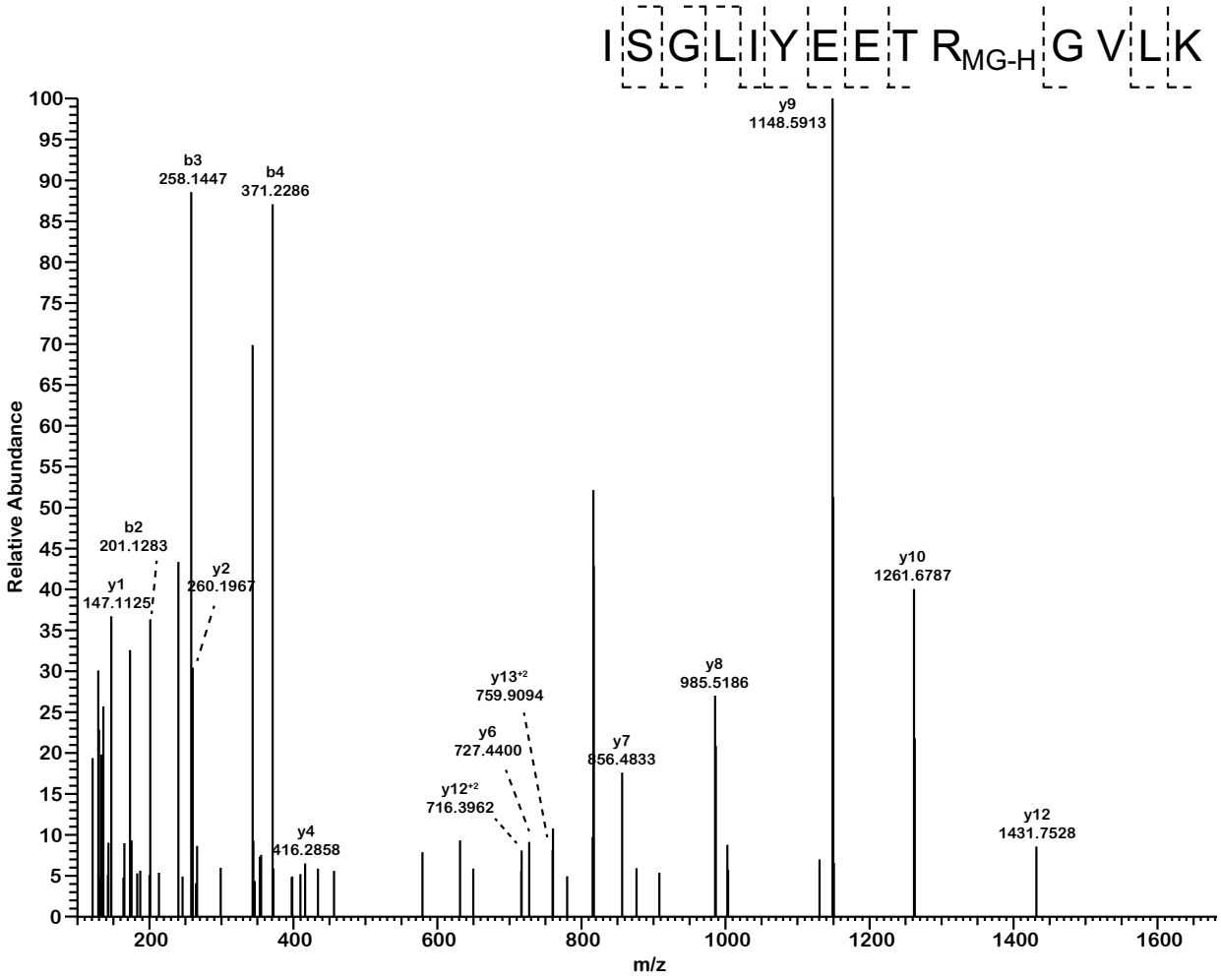

Fig. S37. MS/MS spectra of the MG-H adduct identified at H4R55; Δ 1.35 ppm, retention time of 58.38 min.

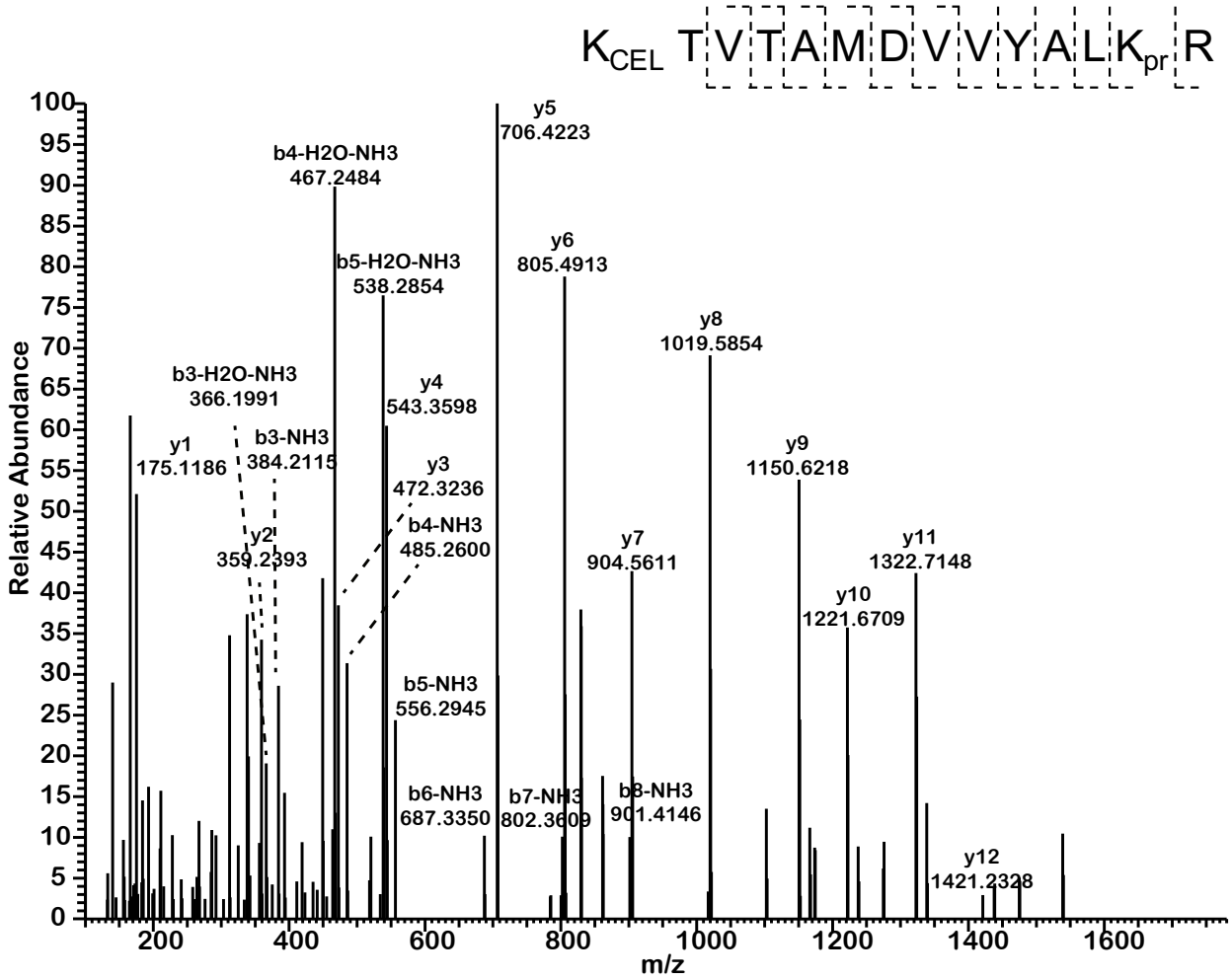

Fig. S38. MS/MS spectra of the CEL adduct identified at H4K79; Δ 5.91 ppm, retention time of 68.98 min.

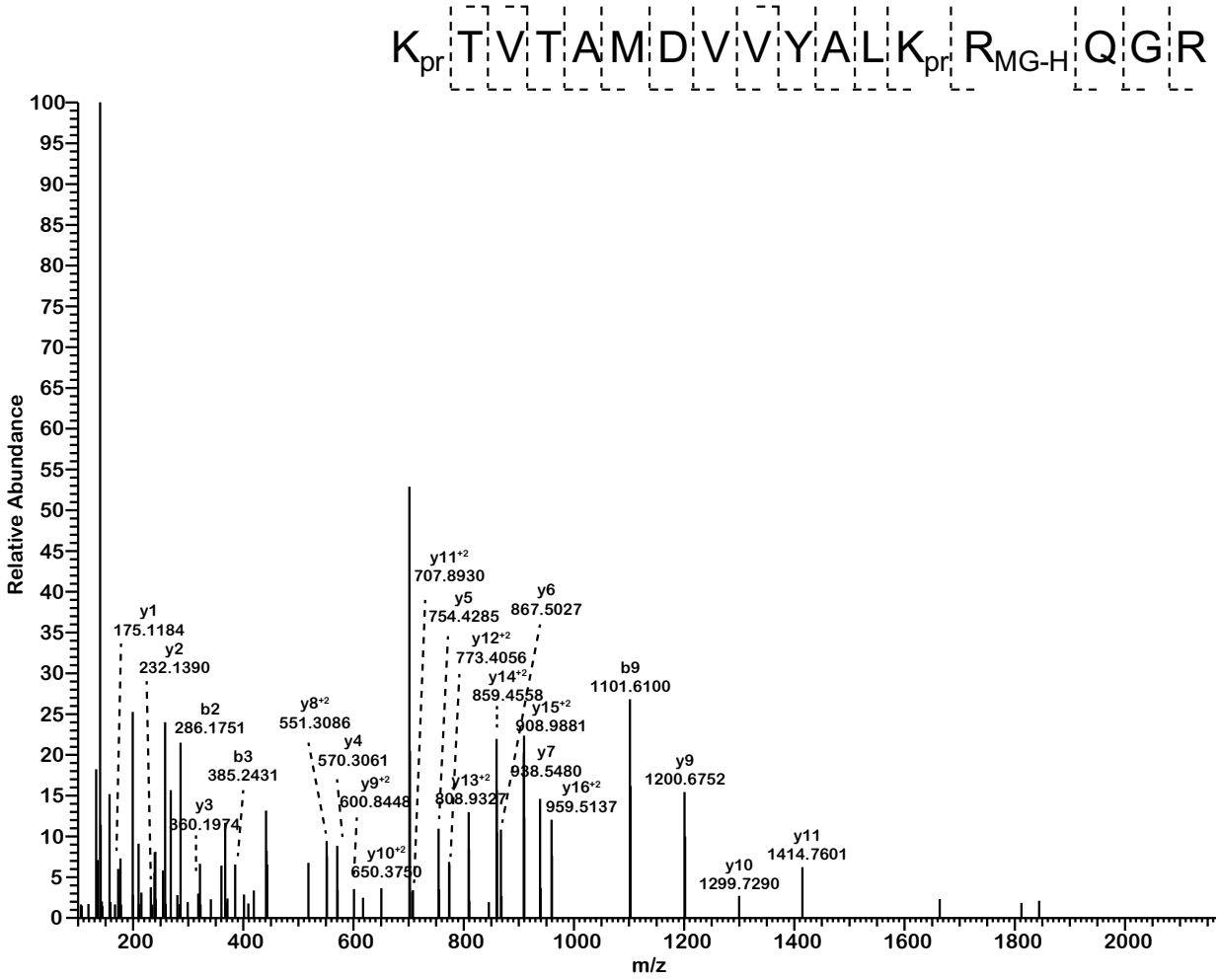

Fig. S39. MS/MS spectra of the MG-H adduct identified at H4R91; Δ 2.56 ppm, retention time of 66.43 min.

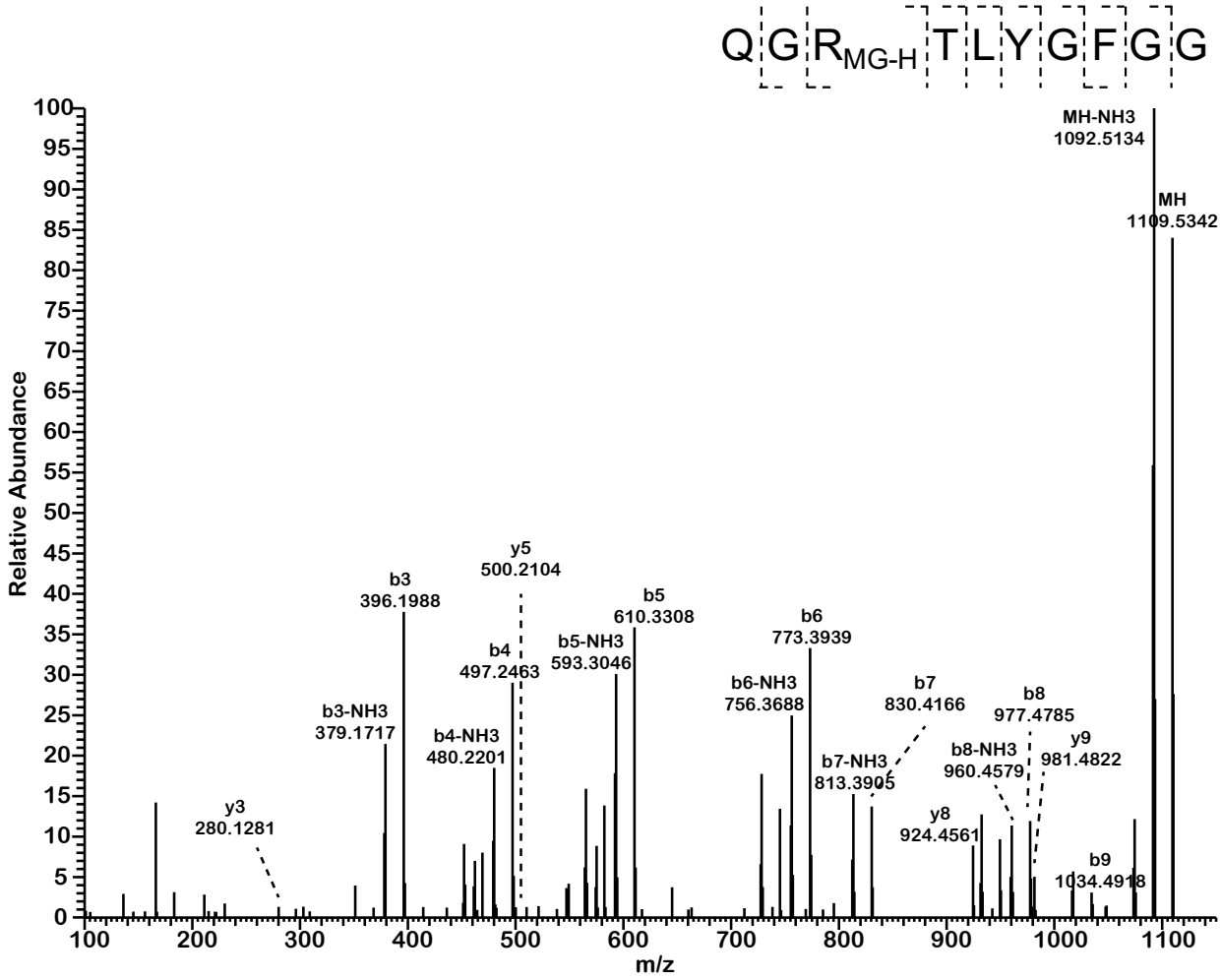

Fig. S40. MS/MS spectra of the MG-H adduct identified at H4R95; Δ 3.33 ppm, retention time of 48.19 min.